Atmosphere

Volume 15 Number 3 1977

Canadian Meteorological Society
Société Météorologique du Canada

Atmosphere

Volume 15 Number 3 1977

Contents

ISSN 0004-6973

Canadian Meteorological Societ
Société Météorologique du Canad

Low-Frequency Motions on the Scotian Shelf and Slope

Brian Petrie and Peter C. Smith
Atlantic Oceanographic Laboratory, Bedford Institute of Oceanography, Dartmouth, Nova Scotia

[Original manuscript received 4 October 1976; in revised form 26 January 1977]

ABSTRACT

An examination of current-meter data gathered in 1967/68 on the continental shelf and slope off Nova Scotia has shown that meteorological forcing is an important source of energy. The response of currents to wind forcing is concentrated in a frequency band of 2.5 to 7 days. Daily mean currents of up to 25 cm/s appear to be associated with wind-stress events. The highest correlations between wind and current are for the alongshore components of these variables. Wind-induced currents may have been responsible for an intrusion of slope water onto the shelf which was observed in hydrographic sections from October and December 1968. Long data series (up to 167 days) formed by patching together shorter records demonstrate the existence of distinct low-frequency variability at periods greater than 10 days. Some aspects of these motions suggest the presence of topographic Rossby waves on the shelf and slope. However, spatial and temporal coverage of data are not sufficient to define the sources of this variability.

1 Introduction

Many water types have been identified on the Scotian Shelf and Slope from extensive hydrographic surveys made since the early 1900s. An overall picture of the main components and circulation of these water masses has been given by McLellan (1954, 1957). As the accuracy and resolution of hydrographic measurements continued to improve, the temporal and spatial variability of the shelf and slope waters became increasingly evident. McLellan (1955) found his conclusions about a 20-year warming trend in bottom temperatures over the shelf to be impaired by "non-systematic" replacement of bottom waters. Variability within the slope water region was emphasized by Worthington (1964) who observed a tremendous volume of Labrador water in that region in 1959 compared to that found in 1960. His estimate of a transport of 50×10^6 m^3/s in the offshore branch of the Labrador Current for $8\frac{1}{2}$ months of that year is an order of magnitude greater than that used by McLellan (1957). From brief observations of the erratic movement of parachute drogues, Foote et al. (1965) concluded that flow in the Labrador Slope Water at depths of 300 to 800 m, though generally westward, was highly intermittent for time scales on the order of days. The use of moored instrument arrays

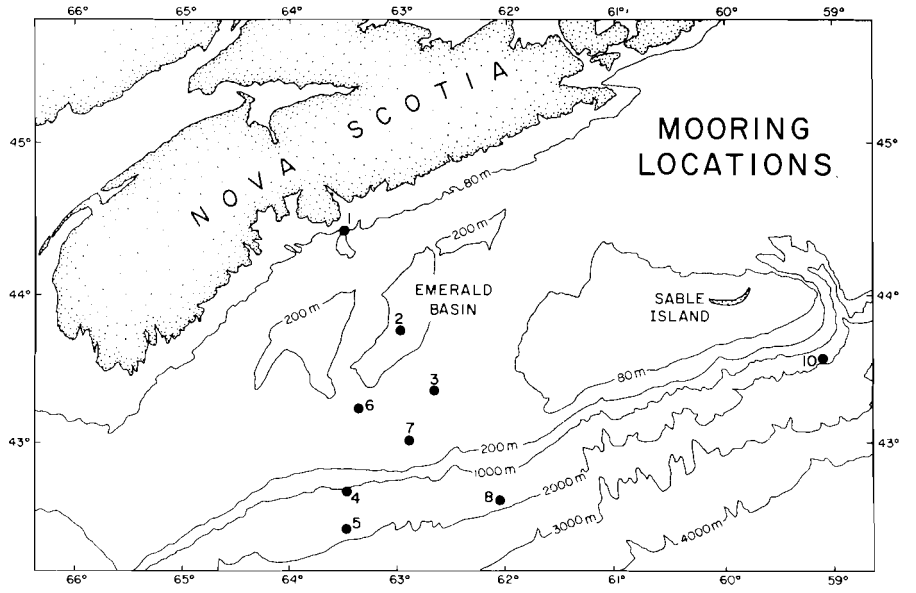

Fig. 1 Mooring sites for the 1967–68 current measurement program.

allowed for the rapid sampling of temperature and velocity fields on the continental shelf and slope. A program to measure these variables was carried out by Bedford Institute of Oceanography in 1967–68 at the sites shown in Fig. 1. Using these data Warner (1970) and Petrie (1974, 1975) have discussed the high-frequency (tides, intertial and internal waves) portion of the spectrum. Low-frequency motions, that is, periods of two days and longer, will be examined here. Two sources of variability, direct meteorological forcing and wave motions such as topographic Rossby waves, will be considered.

The importance of direct meteorological forcing has been demonstrated in experiments conducted on the west and east coasts of the United States. Significant correlations between the alongshore components of wind and current on the continental shelf have been reported by Collins and Pattullo (1970), Huyer and Pattullo (1972), Smith (1974), and Huyer et al. (1975). The response of water to winds was found in the frequency range of 0.4 to 0.16 cpd. Beardsley and Butman (1974) showed that intense wind-forcing events dominate the circulation over the New England continental shelf during winter periods. Boicourt and Hacker (1975) have illustrated intrusions of slope water onto the continental shelf of the eastern United States. They found that a southerly wind forced an offshore Ekman drift in the surface layer requiring a deep return flow. The return flow carried salty slope water onto the shelf giving rise to the possibility that some of the "non-systematic" replacements of bottom waters reported by McLellan (1955) may be due to response to direct wind forcing.

Other more indirect effects of the meteorological disturbances must also be considered such as the free continental shelf waves reported by Cutchin and

Smith (1973). Furthermore, the impingement of the Labrador Current upon the continental slope and the proximity of the strongly meandering Gulf Stream (Hanson, 1970) suggest alternate sources of low-frequency energy. Thompson (1971) found evidence for strong, vertically coherent fluctuations at Site D, a point 50 km south of the shelf break off New England. He interpreted measured periods of two days to two weeks as two-dimensional barotropic Rossby waves driven by the Gulf Stream and propagating northward on the continental rise. Schmitz (1974) conducted an experiment to explore low-frequency motions near the slope-rise junction north of Site D. From 86-day consecutive records, the following important features of the low-frequency motion were deduced:

(1) The low-frequency flow is oriented mainly along isobaths.
(2) The most energetic motions with periods of roughly ten days occur at the slope-rise junction with kinetic energy densities dropping off in either direction. The measured phases between U (eastward current) and V (northward current) are near 180° to the north and south of the junction but 20° to 60° at the junction itself.
(3) Periodograms show energy concentrated at periods from 10 to 18 days and 40 to 60 days but the spectra of kinetic energy are consistently "red."
(4) For periods of 10–18 days significant vertical (100 m separation) and horizontal (25 km separation along isobaths) coherences were reported. Motions were incoherent across contours at the 25 km scale.
(5) Coherence between wind and current ranged to 0.68, just below the 95% confidence limit of 0.70.

Schmitz (1974) concluded that a broad band of barotropic continental shelf waves and the interaction between an incoming barotropic Rossby wave with the continental slope were needed to explain his observations. However, he did not rule out the possibility of atmospheric forcing.

Kroll and Niiler (1976) have developed a model for the propagation of topographic Rossby waves on the continental slope and shelf. Their results indicate that certain "preferred" waves can produce energy densities 8 to 10 times as great as in the deep slope water and can penetrate as far as the 25 m isobath on the shelf before dissipating. Calculations for the New England shelf showed reasonable agreement with Schmitz' (1974) data.

In the next section, the influence of direct meteorological forcing on the circulation over the shelf and slope will be discussed. Because most of the energy in the wind spectrum lies between 2 and 8 days, strong motions at periods greater than 10 days do not appear to be directly driven by the wind. Certain aspects of these longer period motions will be discussed in section 3 followed by a summary of conclusions in section 4.

2 Meteorological forcing

Sable Island Wind Measurements

Lacking wind measurements at the mooring sites, Sable Island was chosen as a source of meteorological data because of its location on the outer continen-

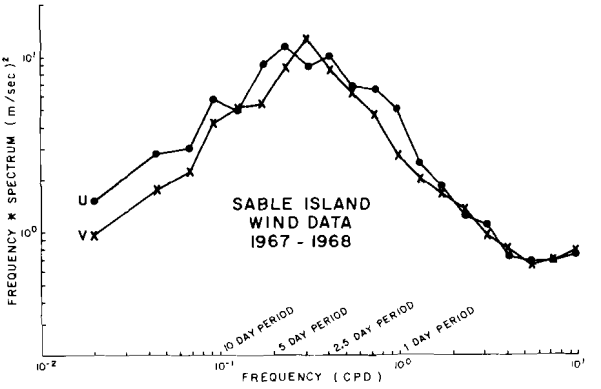

Fig. 2 Sable Island wind spectra computed from 1967/68 data.

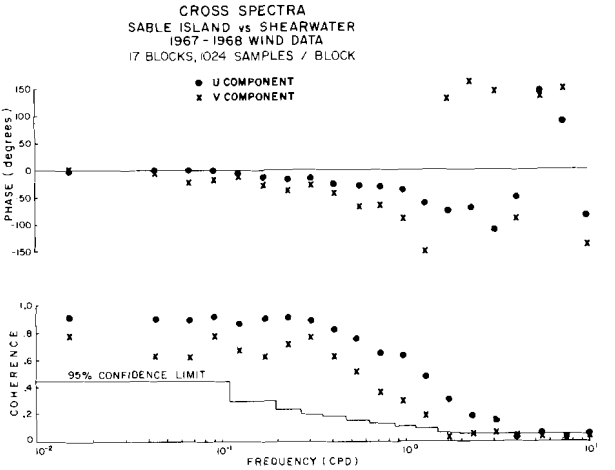

Fig. 3 Cross-spectra results of Sable Island versus Shearwater. The 95% confidence limit for non-zero coherence is from Benignus (1969). For frequencies lower than 1 cpd the size of the points is larger than the 95% confidence limit on the phases.

tal shelf in the same general area as the current measurements. However, the moorings are about 250 km to the west of Sable; thus it must be determined whether the winds at Sable are representative of the winds on the Shelf for this length scale. The Shearwater (near Halifax) weather station is 270 km to the west-northwest of Sable. Spectra and cross-spectra were calculated for the two sites from 1967/68 wind data. A plot of frequency times the spectrum versus frequency for Sable data is shown in Fig. 2. The U component corresponds to the wind blowing toward the east and V to wind blowing toward the north. The spectra have broad peaks centred at periods of three to five days with energy falling off at 1 and 15 days to one-fifth of the peak values. The spectra of the Shearwater data have the same shape but with amplitudes

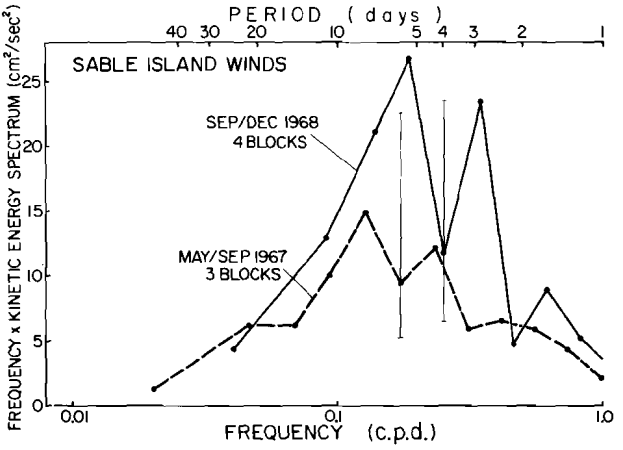

Fig. 4 A comparison of kinetic energy spectra of Sable Island winds for two periods: May/September 1967, and September/December 1968. Vertical bars indicate the 95% confidence limits from Munk et al. (1959).

reduced by a factor of two. In Fig. 3 the cross-spectra of the Sable and Shearwater data are shown. They may be summarized as follows:

Significant coherence	U, period $\geq$ 8 hours
	V, periods $\geq$ 15.4 hours
Coherence > 0.5	U, periods $\geq$ 1 day
	V, periods $\geq$ 1.8 days

From the lowest frequencies to about one cycle per day there is a small but significant phase lag between Sable and Shearwater (a negative lag corresponds to Shearwater leading Sable). At the most energetic periods of 3 to 5 days the lag is equivalent to about 8 hours. Since the mooring sites are also to the west of Sable the winds there would be expected to lead those at the Island by several hours on average. The lag has not been accounted for in the analyses which follow and may be expected to degrade correlations between wind stress and current. The spectral shapes of wind data from Sable and Shearwater are virtually identical and coherence between the two stations is high in the most energetic parts of the spectra indicating that Sable Island measurements are representative of winds over the continental shelf up to length scales of about 300 km. It is reasonable then to compare wind stress as measured at Sable to current meter measurements taken at the sites in Fig. 1.

The current measurements which will be considered fall into two distinctly different time intervals: the summer of 1967 (May/Oct.) and the autumn of 1968 (Sept./Dec.). The summer season was characterized by relatively calm atmospheric conditions, while the latter period contained some of the most intense storms of the entire two-year program. The kinetic energy spectra of Sable Island winds from the two seasons are compared in Fig. 4. Although the

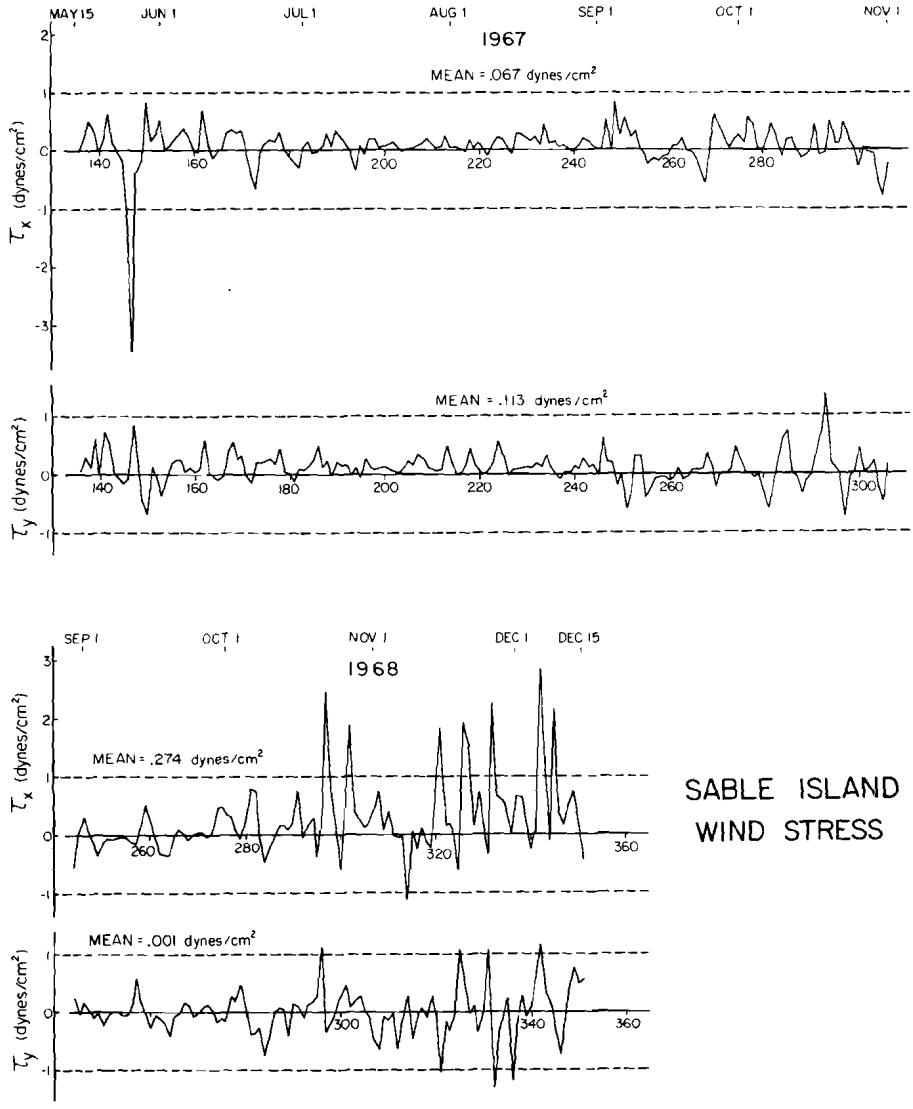

Fig. 5 Sable Island wind stress for May/September 1967 and September/December 1968. Wind stress calculated after Smith and Banke (1975).

distributions of variance with frequency are similar, considerably more total energy is contained in the later period. Fig. 5 shows a comparison of the wind stress components for the two seasons. Only once during the May/October period did a stress component exceed 1 dyne/cm² (1 dyne/cm² = 0.1 N/m²), and its fluctuations were generally less than 0.5 dyne/cm². In contrast, the autumn record, after a relatively quiet September, showed bursts of 1 to 3 dyne/cm² from mid-October to mid-December. Thus, if atmospheric forcing

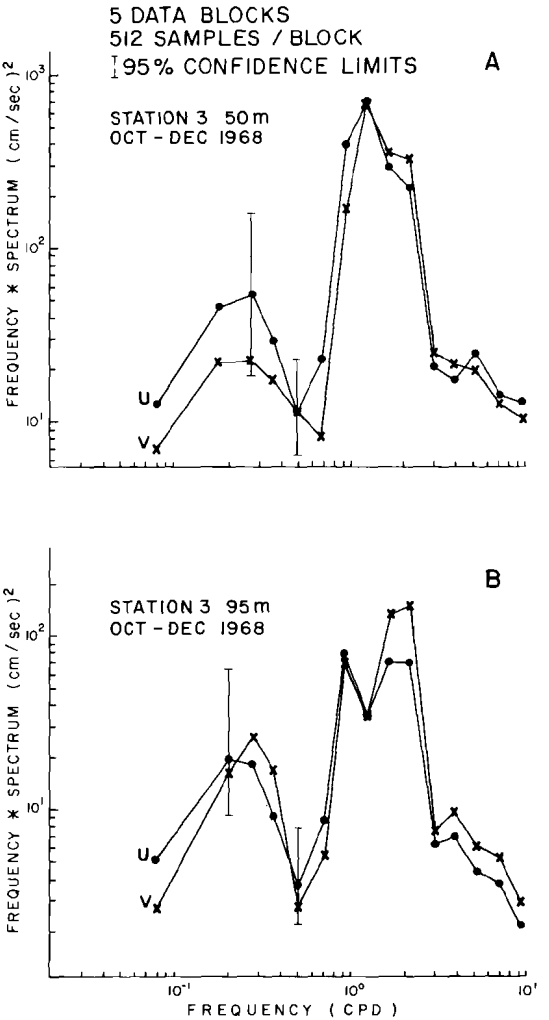

Fig. 6 Frequency times spectrum of current-meter data from Station 3. The 95% confidence limits are from Munk et al. (1959).

be an important mechanism on the shelf and slope, the character of the response should be most evident in records covering September/December 1968. Conversely, if the deep ocean be an important energy source for the shelf the absence of storms in the May/October 1967 period should allow these motions to be detected.

Analysis of October/December 1968 Current Meter-Data, Shallow Banks

The kinetic energy spectra for Station 3 at 50 m and 95 m are shown in Fig. 6. The largest energy values are for frequencies centered at tidal and inertial periods. Also evident in the spectra are broad peaks centred between 2.5 and

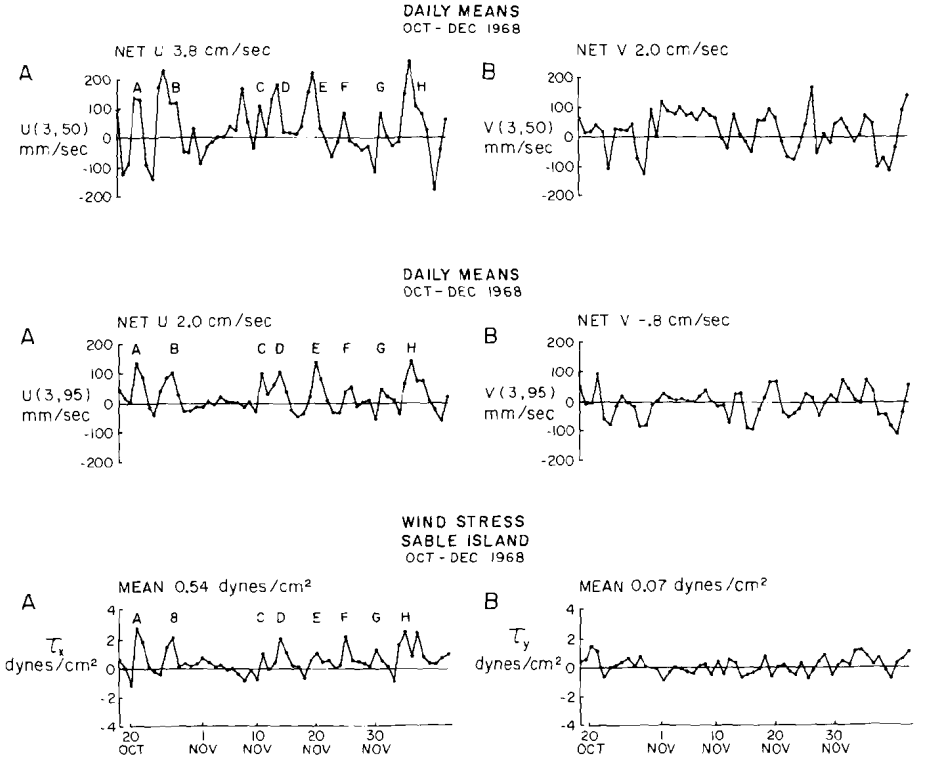

Fig. 7 Daily means of current and wind stress plotted as a function of time. Wind stress was calculated after Smith and Banke (1975).

5.5 days. These peaks, which correspond to the broad peaks in the wind spectra, are significant at the 95% confidence level for the 95 m data but not significant for the 50 m data. Consideration of more examples (Smith and Petrie, 1976) than are given here indicates that this peak is a significant feature of current spectra during windy periods and absent during calmer conditions. Thus it appears that the wind is generating an energetic response in the ocean from periods of 2.5 to 5.5 days.

A more detailed look at the relationship between wind stress and currents is presented in Fig. 7 where daily means of these variables are plotted. Both currents and wind stress have been decomposed into north (V, τ_y) and east (U, τ_x) components. The wind stress was stronger toward the east with a mean of 0.54 dyne/cm^2. The net currents at 50 and 95 m were toward the east at 3.8 and 2.0 cm/s. Throughout the mooring period there were many events of high wind stress labelled A to H in Fig. 7 and corresponding events in the U-component of current labelled similarly. The correlation between τ_x and U is striking especially at 95 m depth. Amplitudes of up to 25 cm/s are reached. However, there are differences such as the peak in current at 50 m depth which occurs just before the event marked C with no corresponding event in

TABLE 1. Correlation and regression coefficients for Station 3 currents and Sable Island winds

$r = \frac{\Sigma(X - \bar{X})(Y - \bar{Y})}{\sigma_x \sigma_y}$ $\quad U = A\tau + B$ $\quad A\left(\frac{\text{cm/s}}{\text{dyne/cm}^2}\right)$ B[cm/s]

$\sigma^2(\ ) = \frac{1}{n}\Sigma[(\ ) - (\bar{\ })]^2$ $\quad U = AU + B$ $\quad A$ [dimensionless] B[cm/s]

Variables	r	r (0.05 level of significance)*	A	B
Oct./Dec. 1968				
$U(50)$, $U(95)$	0.77 (0.72)†	0.27	1.3	1.2
$V(50)$, $V(95)$	0.72 (0.86)		1.0	2.8
$V(50)$, $U(50)$	0.16 (0.53)			
$V(95)$, $U(95)$	0.35 (0.52)			
$U(50)$, τ_x	0.36 (0.48)			
$V(50)$, τ_x	0.05 (0.35)			
$U(95)$, τ_x	0.77 (0.71)		4.3	−0.2
$V(95)$, τ_x	0.22 (0.43)			
Aug./Oct. 1967				
$U(95)$, τ_x	0.48 (0.38)	0.25	4.7	1.3
$V(95)$, τ_x	0.33 (0.35)		3.8	0.2
$V(95)$, τ_y	0.57 (0.33)		5.3	0.2

*Fisher and Yates (1970)
†Low-pass Cartwright filter

wind stress. The correlation between the V-components and τ_x or τ_y is not so striking but note the corresponding steadiness in these variables for the period 1–10 November. The correlation coefficients between these time series have been calculated and are recorded in Table 1. The highest coefficient, 0.77, is between τ_x and U (95 m), the correlation between τ_x and U (50 m) is significant but low and finally the correlations between wind stress and the V-components are not significant at the 95% level. For cases when the correlation is high the linear regressions have been calculated and are tabulated in Table 1. Also shown are the correlation coefficients between the current components at the same and at different depths. The correlations between like components at 50 and 95 m are high (0.77 for U, 0.72 for V) while between different components at the same depth the coefficient is low but significant (0.35) at 95 m and not significant (0.16) at 50 m. Visually, these relationships are shown in the scatter plots of Fig. 8. The slopes of the linear regressions of U (50) versus U (95) and V (50) versus V (95) were 1.3 and 1.0 respectively indicating that the response is nearly barotropic.

Hydrographic sections (de la Ronde, 1972) were available at the time the mooring went in and when it came out of the water. The location of the hydrographic stations and the contours of salinity are shown in Fig. 9. To the left of the diagram is the section taken in October when Station 3 was laid. There was no 35‰ salinity water in Emerald Basin and the 33.5‰ isohaline intersected the shelf break. To the right of the diagram is the section taken in

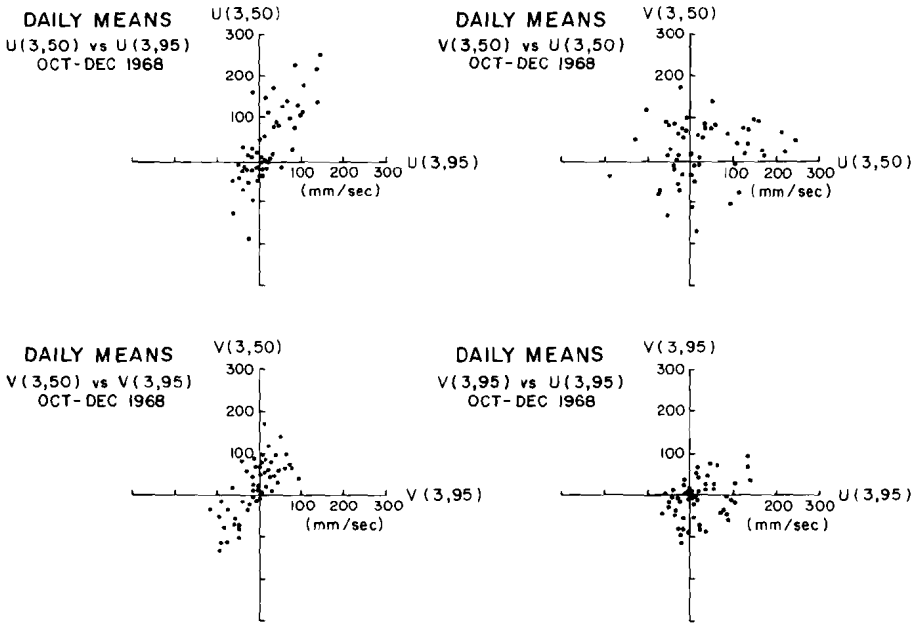

Fig. 8 Scatter plots of daily mean velocity components at Station 3.

December when mooring 3 was recovered. There was a substantial quantity of $35^0/_{00}$ water in the Basin and the $34^0/_{00}$ isohaline lay over the outer continental shelf. These observations indicate an intrusion had occurred. During this period the mean alongshore wind stress was 0.54 dyne/cm^2 and mean V-component of current at 50 m was onshore at 2.0 cm/s. This is suggestive of the mid-depth type of intrusion seen by Boicourt and Hacker (1975). However, note from Table 1 that the correlation of τ_x and V (50) is quite low and that during the period 1–10 November when τ_x was nearly zero V (50) was about 10 cm/s onshore.

After these correlations were completed it was realized that the daily mean is not the best choice of filter which could have been made. A better choice would have been a low-pass Cartwright filter. Such a filter (100% power passed at periods of one day and longer, less than 5% passed at inertial periods) was applied to the same data sets shown in Table 1 after the tides had been removed. The correlations from this filtered data are shown in brackets in Table 1. Most correlations are enhanced, the important change being a significant positive value between τ_x and V at both depths. This indicates that a positive τ_x could drive a mid-depth intrusion of slope water.

Several characteristics of the water's response to wind forcing suggest the presence of continental shelf waves. Gill and Schumann (1974) have discussed the generation of such waves by the wind. When their model was applied in the present case velocity amplitudes and periods for the shelf waves were consistent with observations. However, their model was found wanting

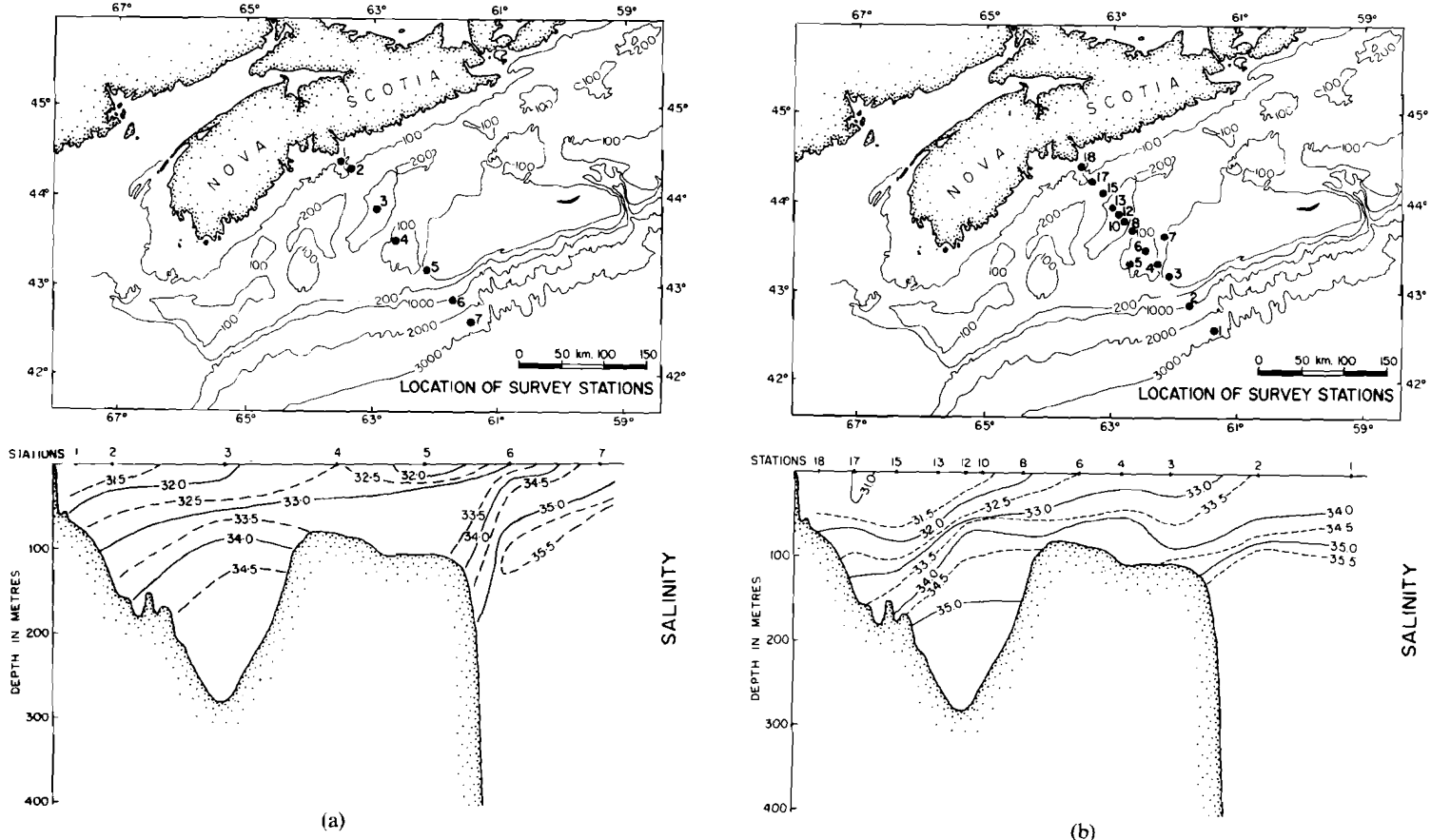

Fig. 9 Salinity contours in parts per thousand for hydrographic sections taken on 20–21 October 1968 (a), and 16–17 December 1968 (b).

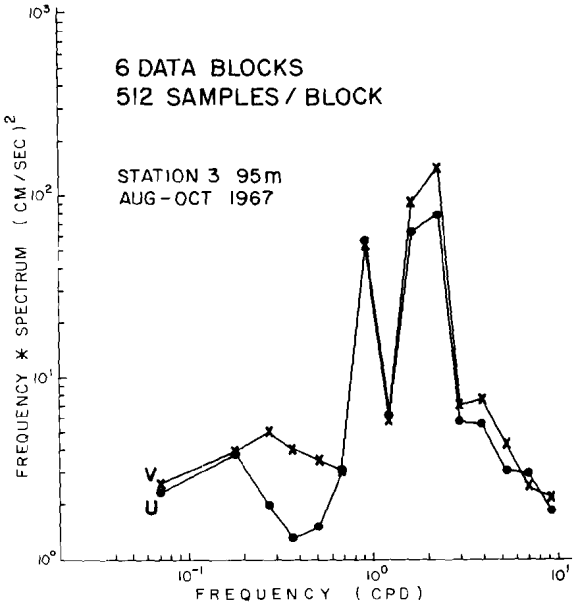

Fig. 10 Frequency times spectrum of current meter data from Station 3, 95 m.

in several aspects. Moreover, other features of the data did not have shelf wave characteristics. Gill and Schumann's (1974) condition for the neglect of the surface divergence is not met for the Scotian Shelf (the parameter [their notation] ϵ^2 should be much less than 1 whereas $\epsilon^2 = 0.4$ in our case). Their exponential model of the topography is a poor fit to the depth variations on the Scotian Shelf. The ratio U/V of the velocities for continental shelf waves should be proportional to f/ω, where f is the Coriolis parameter and ω is the wave frequency. In the band 1.5 to 12 days the ratio should range from 2 to 17; however, the data at 50 and 95 m showed the ratio varied from 0.7 to 1.7 in the cases (9 of 12) where the coherence between U and V was above the 95% confidence limit. The cospectra for these waves should be zero but when there was significant coherence all measured cospectra were positive. Put another way, for continental shelf waves the U component should lead V by $\pi/2$ radians whereas in all instances V was leading U. A more detailed model, especially one which accounts for the complicated topography of the Scotian Shelf, than Gill and Schumann's (1974) must be examined to determine how much of the low frequency variance seen in these data may be attributed to continental shelf waves.

Current-Meter Data, Shallow Banks (May/October 1967)

In Fig. 10 the spectra of currents from Station 3, 95 m, are shown for the period August/October 1967 when conditions were calm. Compared to the spectra in Fig. 6 at the same depth the reduction of energy in the band 2.5 to 10 days is by a factor of 5 to 10. Moreover, the inertial peak is reduced by a factor

TABLE 2. Records considered for low-frequency analysis

Station	Location	Bottom metres	Instrument Depth metres	Period	Record Length days
4	slope-rise	1015	150, 980	Sept./Dec. 1968	55, 78
8	rise	1550	1500	Sept./Oct. 1968	33
2	Emerald Basin	278	50, 250	May/Oct. 1967	167
			95, 250	Sept./Dec. 1968	97

of 6. But notice the diurnal and semidiurnal peaks are almost unchanged as expected since the tides on this portion of the shelf are mostly barotropic (Petrie, 1975). Data (not shown) at 50 m May/July 1967 show a similar reduction in the low-frequency portion of the spectra and a reduction of the inertial peak by a factor of 10. The contrast between these observations confirms that meterological forcing is responsible for the high energy at periods of about 2 to 10 days.

Even though conditions were relatively calm for the period August/October 1967 significant correlations were found between current at 95 m and wind stress and are given in Table 1. Correlations for other Station 3 data were calculated but were not significant at the 0.05 level.

3 Longer period motions

Direct atmospheric forcing of the shallower shelf water (typified by Station 3) at periods from 2 to 10 days appears to be well established from the results of the previous section. In contrast, the following analysis will be focussed on very low-frequency fluctuations with periods greater than 10 days. In order to look at the lowest frequencies, emphasis will be placed on the longest available records from the 1967/68 mooring program. The records to be discussed range from 33 to 167 days in length and are listed in Table 2.

The data consist of three records from two moorings on the continental slope and rise during the stormy autumn season (Sept./Dec. 1968) plus two records from a shelf mooring during both the quiet summer period (May/Oct. 1967) and the autumn season. Unfortunately, the 67/68 experiment was not specifically designed to look at low-frequency motion, so that the data coverage in both space and time is insufficient to define adequately the character of fluctuations of 10- to 40-day duration. Therefore the question of energy sources for these motions must remain unanswered for the present. However, it is possible to demonstrate the existence of distinct low-frequency variability and make some general comments about its nature. To investigate the lowest frequency bands, the data will be analyzed in only a few large data blocks thereby sacrificing some stability in the spectral estimates.

Slope Stations (Sept./Dec. 1968)

Deep current measurements on the continental slope of Nova Scotia exhibit low-frequency variability similar to that found by Schmitz (1974) and

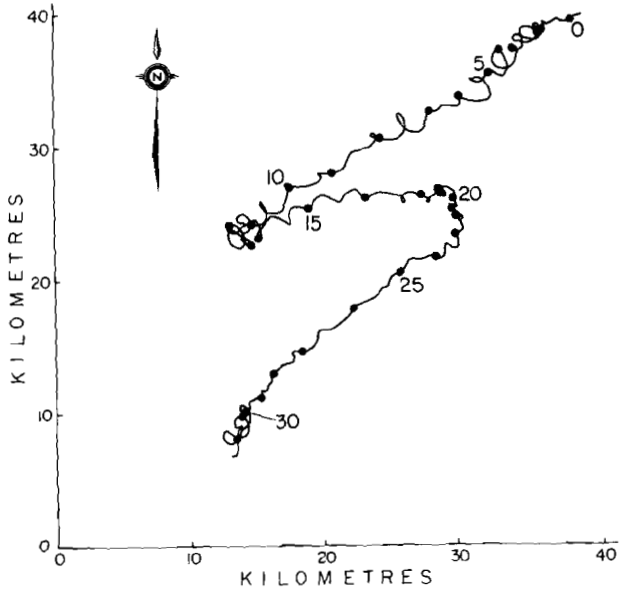

Fig. 11a Progressive vector diagram for Station 8 currents at 1500 m, September/December 1968 (from Grant and Reiniger, 1971). Numerals indicate number of days from start of record.

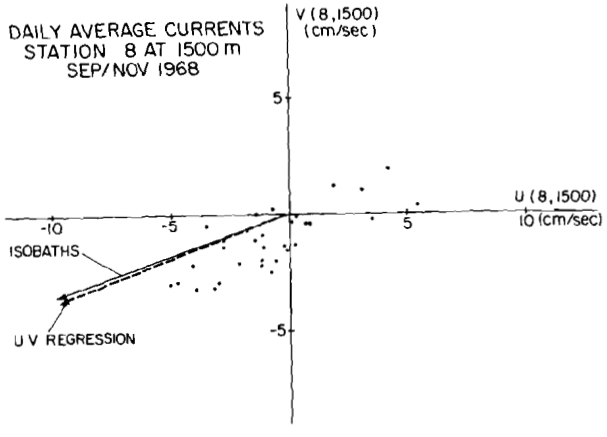

Fig. 11b Correlation of daily mean velocity components at Station 8, 1500 m, September/December 1968.

Thompson (1971) for the New England continental rise and slope. The most dramatic example of this behaviour is the progressive vector diagram of currents at 1500 m for Station 8 shown in Fig. 11(a). Twice during the 33-day record, the current reversed distinctly, separating the record into three segments of nearly rectilinear flow. A correlation of the daily averaged U (east) and V (north) components has a coefficient of 0.77 (significant above the 99.9% level, Fisher and Yates, 1970) and gives a regression axis which deviates from the local isobaths by less than 1° [Fig. 11(b)]. The estimated

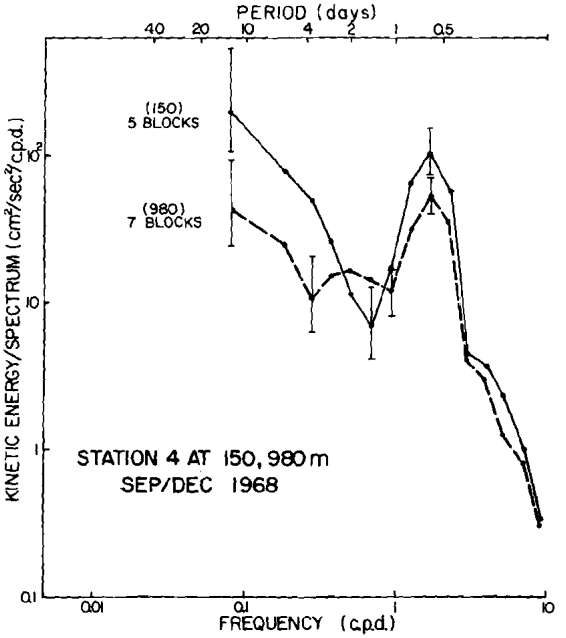

Fig. 12 Kinetic energy spectra for Station 4 currents at 150, 980 m in September/December 1968. 95% confidence limits from Munk et al. (1959).

error involved in determining the direction of the isobath at that location is ±5° so the deviation is not significant.

The longest records from the slope region (55, 78 days) were taken at Station 4 during the fall of 1968. The kinetic energy spectra at 150 m and 980 m are shown in Fig. 12. At high frequencies the tidal and inertial bands are quite energetic while the low-frequency spectra are distinctly "red." In addition, there are indications of a secondary peak centred at a period of two days in the spectrum of the deeper record but it is not significant because of the poor stability of the spectral estimates. The correlation of the two velocity components at the bottom meter [shown in Fig. 13(a)] gives a regression axis which is rotated from the direction of the local isobaths by roughly 6° in the clockwise sense. This difference is consistent with Schmitz's (1974) results and is marginally above the estimated direction errors at Station 4 (±5°); however, the correlation coefficient of 0.15 is not significant at the 0.1 level (Fisher and Yates, 1970) and contrasts to the value of −0.6 found by Thompson (1971) at Site D. The lack of a strong correlation between U and V signifies that the dynamics are more complex than those of a single topographic Rossby wave propagating shoreward and partially reflecting from the continental slope. Fig. 13(b) shows the coherence and phase between velocity components at the 980 m sensor. There are no significant coherences at the 95% level for the lowest frequencies although a value greater than 0.6 is found for periods slightly above 10 days. The phase estimate at this frequency (30° ± 20°) is consistent with the range (20°–60°) measured by Schmitz (1974) at the slope-

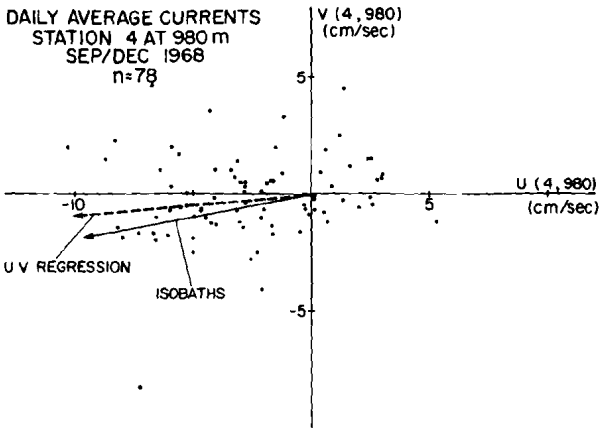

Fig. 13a Scatter plot for daily mean velocity components at Station 4, 980 m, September/December 1968.

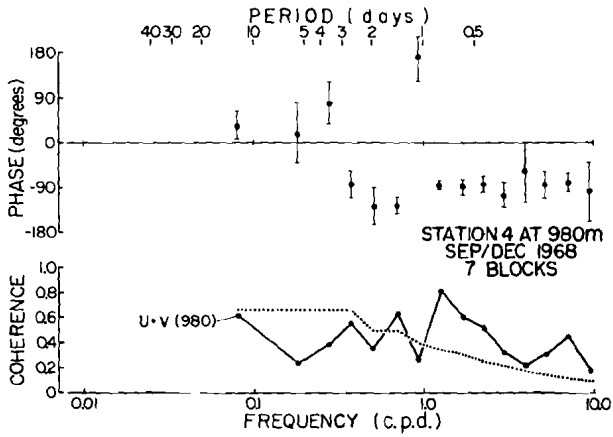

Fig. 13b Coherence and phase between velocity components at Station 4, 980 m, September/December 1968. Positive phase means U leads V. ···· 95% confidence level for non-zero coherence (Benignus, 1969). Vertical bars indicate the 95% confidence level for phase (Jenkins and Watts, 1968).

rise junction. This comparison is significant since Smith and Petrie (1976) have demonstrated that the slope-rise junction along 63°30'W south of Halifax is located somewhere between the 1000 m and 1500 m isobaths. At higher frequencies, a significant coherence does occur at a period near two days where there seemed to be some concentration of energy in the kinetic energy spectrum.

Finally, it is of interest to explore the possibility of atmospheric forcing of the deep slope waters by examining the correlation between current and alongshore wind at Station 4. Fig. 14 shows the coherence and phase between currents at 980 m and the eastward wind component at Sable Island. In the

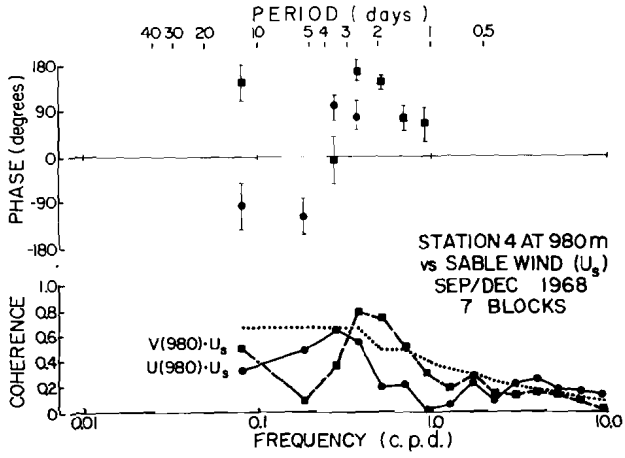

Fig. 14 Coherence and phase between Station 4 currents at 980 m and eastward Sable Island winds, September/December 1968. Positive phase means current leads. ···· 95% confidence level for coherence (Benignus, 1969). Vertical bars indicate the 95% confidence level for phase (Jenkins and Watts, 1968). Absence of phase estimate means error exceeds ±180°.

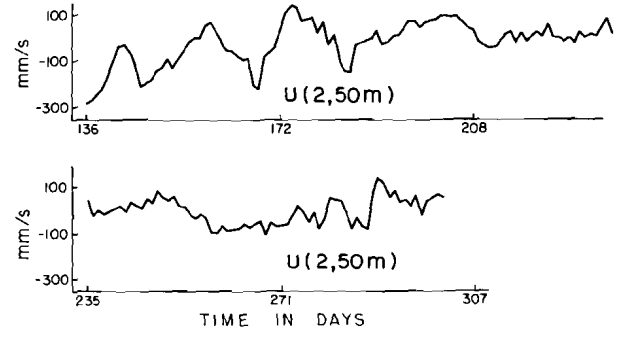

Fig. 15 Daily averaged eastward current at Station 2, 50 m, May/October 1967. Julian day number is indicated.

lowest frequency band, the highest coherence (0.50) occurs between V (980) and U_s with a phase near 180° (i.e. a negative correlation), but is well below the 95% level. Schmitz (1974) reported similar levels of coherence at low frequencies between deep onshore currents and alongshore wind. For periods of 2 to 4 days, this coherence is significant and the phase is again close to 180°. This indicates that during the stormy fall season alongshore winds may be forcing deep currents on the slope with winds *to the east* associated with *offshore* flow at depth over a broad range of frequencies.

Shelf Moorings (May/October 1967)

Some of the measurements made on the Scotian Shelf during the quiet summer of 1967 also indicate strong low-frequency fluctuations. For example, Fig. 15 shows the 167-day record of daily averaged eastward velocity at a

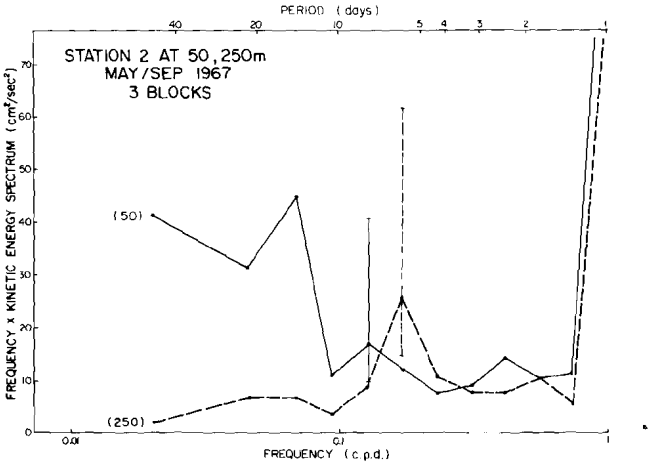

Fig. 16a Kinetic energy spectra at Station 2, 50 and 250 m, May/September 1967. Vertical bars indicate the 95% confidence limits from Munk et al. (1959).

depth of 50 m from Station 2 in Emerald Basin. The 15–20 day oscillations evident in this component, particularly over the earlier portion of the record, do not directly correspond to any major wind stress events as indicated in Fig. 5 where most of the variability occurs at substantially higher frequency. Furthermore, according to the regressions computed for Station 3, wind-driven currents of the order of 10 cm/s require surface stresses of 3 dyne/cm^2, none of which are evident in Fig. 5 after day 148. It is not reasonable to expect that the smaller stresses driving a deeper body of water would produce a significantly stronger response.

Fig. 16(a) shows a variance-conserving plot of the kinetic energy spectra for currents measured at Station 2 during May/September 1967. (Notice that the block size has been adjusted so that only the summer months are included.) Most of the low-frequency variance at the 50 m level is concentrated at periods greater than 10 days and there is a very weak local maximum in these bands. Due to coarse resolution and poor stability individual peaks cannot be isolated. However, it is clear that, at least for the 50 m depths, there is a significant amount of energy contained at periods greater than 10 days, which is separated from that found in the band between 2 and 8 days by a spectral gap centred at 10 days. Also notice that for the bottom record a distinct peak occurs at a period slightly greater than 5 days. A secondary maximum in the 50-m spectrum occurs at roughly 7 days.

To contrast this behaviour, the kinetic energy distribution at similar depths for the September/December 1968 period is displayed in Fig. 16(b). In this plot the high variance for the shallow sensor at 10- to 20-day periods is no longer present. Rather the dominant peaks occur at meteorological time scales (5–8 days). Comparing the total kinetic energy in the range from 2 to 10 days for Stations 2 (Fig. 16) and 3 (Figs. 6 and 10) indicates levels of 2 to 5 times higher in

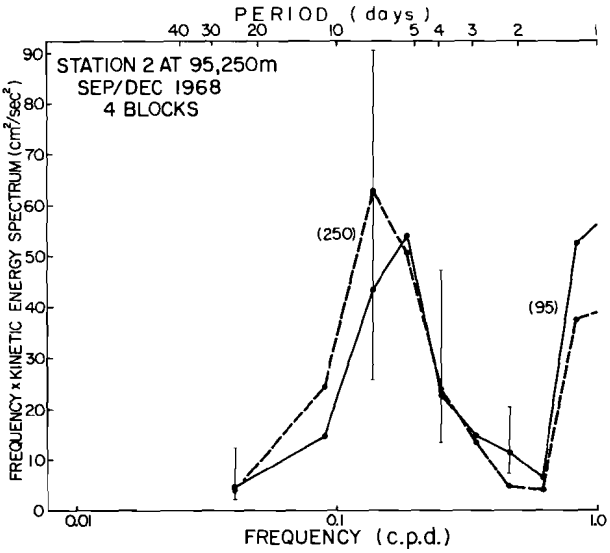

Fig. 16b Kinetic energy spectra at Station 2, 95 and 250 m, September/December 1968. Vertical bars indicate the 95% confidence limits from Munk et al. (1959).

the fall season, which is consistent with the magnification in the wind field variance. Thus the low-frequency energy at 50 m in Fig. 16(a) appears to be a departure from the direct wind-driven response.

Various coherences between velocity components at Station 2 for May/September 1967 are shown in Figs 17 and 18. In the lowest three frequency bands, some high coherences are found but only one exceeds the 95% confidence level. The phase between U and V approaches $-180°$ at the lowest frequencies giving nearly rectilinear flow. This implies an offshore (southward) momentum flux in these bands and contrasts with that in the wind-driven band which is oppositely directed. At atmospheric frequencies, the coherence estimates are variable with some significant values near 2- and 7-day periods. In contrast, Fig. 19 shows similar calculations for September/December 1968 in which a broad band of significant coherences appears between 2 and 10 days with generally lower values at periods greater than 10 days.

Comparison of the current-meter statistics at Station 2 from the two different seasons suggests that the source of low-frequency energy in summer might not be atmospheric for two reasons:

(1) the low level of driving wind stresses through the entire period, and
(2) the dip in the spectrum of kinetic energy [Fig. 16(a)] near 10-day periods separating some fairly coherent motions at lower frequencies from those in the atmospheric bands.

An alternate candidate for the energy source is the low-frequency topographic waves on the slope suggested by the similarity between Station 4 results and

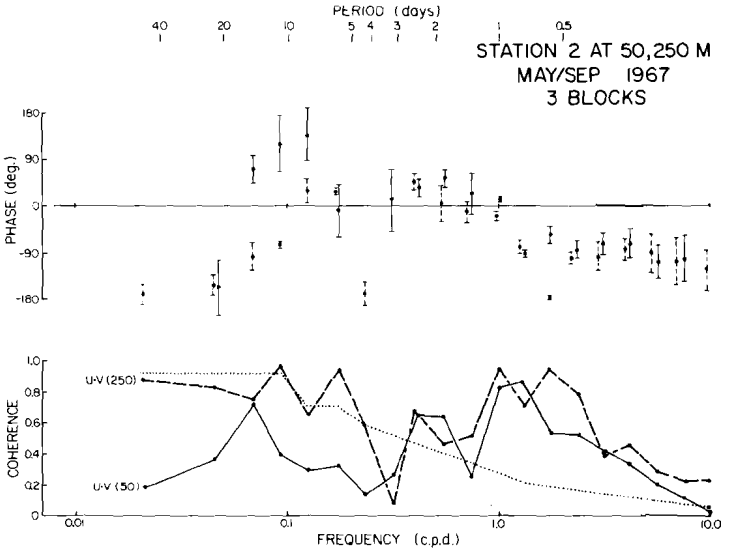

Fig. 17 Coherence and phase between eastward (U) and northward (V) currents at Station 2, 50 and 250 m, May/September 1967. Positive phase means U leads V. ····· 95% confidence level for coherence (Benignus, 1969). Vertical bars indicate the 95% confidence level for phase (Jenkins and Watts, 1968). Absence of phase estimate means error exceeds ±180°.

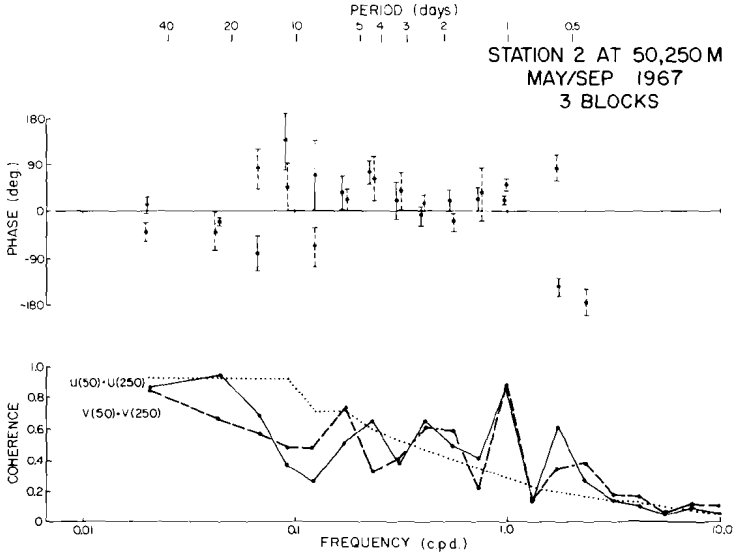

Fig. 18 Vertical coherence and phase between Station 2 velocity components at 50 and 250 m, May/September 1967. Positive phase means upper sensor leads. ····· 95% confidence level for coherence (Benignus, 1969). Vertical bars indicate the 95% confidence level for phase (Jenkins and Watts, 1968). Absence of phase estimate means error exceeds ±180°.

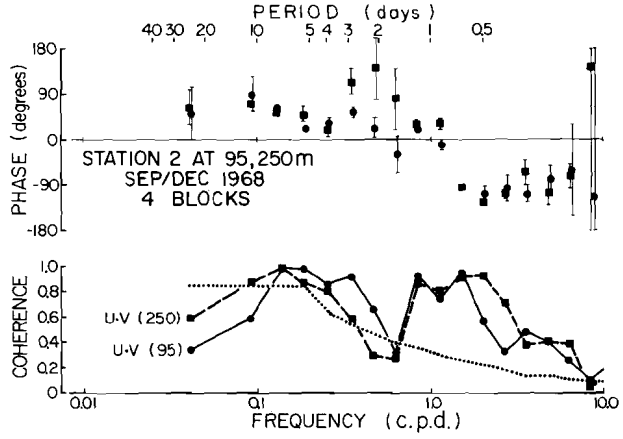

Fig. 19 Coherence and phase between eastward and northward currents at Station 2, 95 and 250 m, September/December 1968. Positive phase means U leads V. ····· 95% confidence level for coherence (Benignus, 1969). Vertical bars indicate the 95% confidence level for phase (Jenkins and Watts, 1968). Absence of a phase estimate means the error bars exceed ±180°.

Schmitz' (1974) data. A recent model for the propagation of barotropic Rossby waves onto exponential shelf topography [Kroll and Niiler (1976)] indicates that certain waves may be transmitted preferentially onto the shelf leading to energy densities which are enhanced by factors of order 10. For realistic estimates of dissipation, model waves penetrate to the 25 m isobath before they are fully damped. The observed tendency toward offshore momentum flux at Station 2 in the lowest frequency bands (see Fig. 17) is consistent with shoreward propagating topographic waves. However, the disparity in energy levels at 50 and 250 m indicates that a significant part of these motions is not barotropic. Moreover, the coherences between Station 2 current and Sable Island wind components (Fig. 20) cast doubt on this hypothesis. The high values at low frequencies are comparable to those among the current components alone. Therefore no definite conclusion is possible regarding the origin of low-frequency variability on the shelf.

4 Conclusion

In summation the analysis of the 1967/68 current-meter data has revealed the following important features of low-frequency motion on the Scotian Shelf and Slope:

(1) On average Sable Island is a good indicator of meteorological conditions over the Scotian Shelf. In general, winds at the mooring sites should lead Sable.

(2) The currents on the shallow banks respond with a spectral peak in a frequency band of from 2.5 to 7 days to the broader band (1 day to 2 weeks) forcing of the winds. During periods of low wind stress the

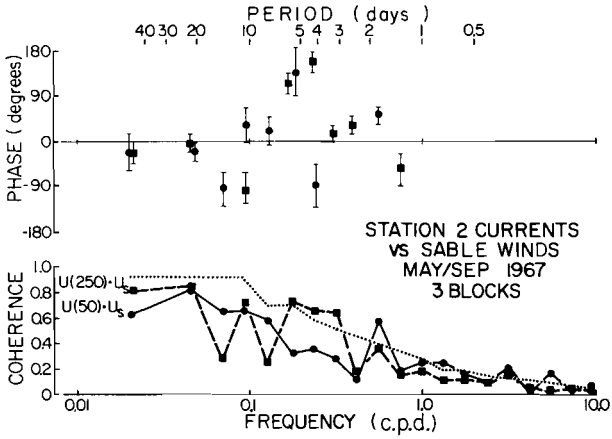

Fig. 20 Coherence and phase between eastward current at Station 2 and Sable Island wind, May/September 1967. Positive phase means current leads. ···· 95% confidence level for coherence (Benignus, 1969). Vertical bars indicate the 95% confidence level for phase (Jenkins and Watts, 1968). Absence of phase estimate means error exceeds ±180°.

current peak is reduced by a factor of 5 to 10. The inertial period energy behaves similarly.

(3) The correlation between alongshore wind stress and currents can be significant with values as high as 0.77. The highest correlations are for alongshore stress and the current near the bottom.

(4) Daily mean currents of up to 25 cm/s appear to be associated with wind stress events.

(5) The response to wind forcing on the shallow banks is nearly barotropic with like components of current at different depths being highly correlated.

(6) With a mean alongshore wind stress of 0.54 dyne/cm^2 to the east during October-December 1968, the mean V component at Station 3, 50 m, was onshore at 2.0 cm/s. Hydrographic sections indicate that during this period an intrusion of slope water onto the shelf and into Emerald Basin occurred.

(7) Deep currents on the continental slope exhibit distinct low-frequency motion oriented primarily along isobaths. The regression axes for daily average currents are generally consistent with those found by Schmitz (1974) but correlations are not always statistically significant over the short records.

(8) Coherence between velocity components near the bottom over the slope is generally high but not significant at the 95% level for periods greater than 2 days.

(9) Coherences between deep slope currents and alongshore winds at Sable Island show marginal significance at periods from 2 to 4 days, where it appears that *eastward* winds are associated with *southward* currents.

(10) Energetic low-frequency motions also occur at Station 2 on the shelf. A comparison of spectra reveals high kinetic energy at 50 m for periods greater than 10 days during a quiet summer period (May/Sept, 1967) contrasting to a dominant peak at meteorological time scales (2 to 10 days) during a stormy autumn season (Sept./Oct. 1968).

The low-frequency summertime oscillation appears to be vertically coherent and in phase with the flow at 250 m although its amplitude is greatly reduced at depth.

(11) Coherences between velocity components at a single depth for periods greater than 10 days tend to be higher during May/October than September/December, but for periods from 2 to 10 days there are significant coherences in both seasons with highest levels obtained in September/December. Measured phases between U and V at Station 2 in summer imply an offshore momentum flux in the lowest frequency bands, particularly at 250 m. This feature is consistent with shoreward propagating topographic Rossby waves and contrasts with the momentum flux in the wind-driven band which is oppositely directed.

(12) Despite low wind-stress levels during the summer months, atmospheric forcing cannot be ruled out as a source of the low-frequency oscillations at Station 2 in light of the high coherences between currents and Sable Island wind. Therefore the origin of this variability remains an open question.

References

BEARDSLEY, R.C. and B. BUTMAN. 1974. Circulation on the New England continental shelf: response to strong winter storms. *Geophys. Res. Lett.* **1**, no. 4: 181–4.

BENIGNUS, V.A. 1969. Estimation of coherence spectrum and its confidence interval using Fast Fourier Transform. IEEE Trans. on Audio and Electroacoustics, AU-17, no. 2: 145–50.

BOICOURT, W. and P. HACKER. 1975. Circulation on the Atlantic continental shelf of the United States, Cape May to Cape Hatteras. Contribution 218, Chesapeake Bay Institute, the Johns Hopkins University.

COLLINS, C.A. and J.G. PATTULLO. 1970. Ocean currents above the continental shelf off Oregon as measured with a single array of current meters. *J. Mar. Res.* **28**, no. 1: 51–68.

CUTCHIN, D.L. and R.L. SMITH. 1973. Continental shelf waves: low-frequency variations in sea level and currents over the Oregon continental shelf. *J. Phys. Oceanog.* **3**, no. 1: 73–82.

DE LA RONDE, M.S. 1972. Temperature, salinity and density distributions of the Scotian shelf, 1965–1971. *Bedford Institute Report*, Data Series/BI-D-72-6, 55 pp.

FISHER, R.A. and P. YATES. 1970. *Statistical tables for biological, agricultural and medical research*. London: Oliver and Boyd, 146 pp.

FOOTE, T.R.; C.R. MANN; and A.B. GRANT. 1965. Oceanographic results of cruise S-64 between the Scotian Shelf, Grand Banks of Newfoundland and the Gulf Stream. *Bedford Institute Report* 65–8, 40 pp.

GILL, A.E. and E.H. SCHUMANN. 1974. The generation of long shelf waves by the wind. *J. Phys. Oceanogr.* **4**(1): 83–90.

GRANT, A.B. and R.F. REINIGER. 1971. Current meter and thermograph observations on the Scotian Shelf – 1968. *Bedford Institute Report*, AOL Data Series 1971-6-D, 395 pp.

HANSON, D.V. 1970. Gulf Stream meanders between Cape Hatteras and the Grand Banks. *Deep-Sea Res.* **17**: 495–511.

HUYER, A. and J.G. PATTULLO. 1972. A comparison between wind and current observations over the continental shelf off Oregon, summer 1969. *J. Geophys. Res.* **77**, no. 18: 3215–20.

———. B.M. HICKEY; J.D. SMITH; R.L. SMITH; and R.D. PILLSBURY. 1975. Alongshore coherence at low frequencies in currents observed over the continental shelf off Oregon and Washington. *J. Geophys. Res.* **80**, no. 4: 3495–3505.

JENKINS, G.M. and D.G. WATTS. 1968. *Spectral analysis and its applications*. San Francisco: Holden-Day, 525 pp.

KROLL, J. and P.P. NIILER. 1976. The transmission and decay of barotropic topographic Rossby waves incident on a continental shelf. *J. Phys. Oceanogr.* **6** (4): 432–50.

MC LELLAN, H.J. 1954. Temperature-salinity relations and mixing on the Scotian Shelf. *J. Fish. Res. Board Can.* **11**, no. 4: 419–30.

———. 1955. Change in bottom temperatures on the Scotian Shelf. *J. Fish. Res. Board Can.* **12**, no. 3: 375–86.

———. 1957. On the distinctness and origin of the slope water off the Scotian Shelf and its easterly flow south of the Grand Banks. *J. Fish. Res. Board Can.* **14**, no. 2: 213–39.

MUNK, W.H.; F.E. SNODGRASS; and M.J. TUCKER. 1959. Spectra of low-frequency ocean waves. *Bull. of Scripps Inst. of Oceanogr.* **7**, no. 4: 283–362.

PETRIE, B. 1974. Surface and internal tides on the Scotian Shelf and Slope. Ph.D. thesis, Dalhousie Univ., Halifax, N.S., 152 pp.

———. 1975. M2 surface and internal tides on the Scotian Shelf and Slope. *J. Mar. Res.* **33**, no. 3: 303–23.

SCHMITZ, W.J., 1974. Observations of low-frequency current fluctuations on the continental slope and rise near Site D. *J. Mar. Res.* **32**, no. 2: 233–51.

SMITH, P.C. and B. PETRIE. 1976. A proposal to study the dynamics at the edge of the Scotian shelf. Bedford Institute of Oceanography Contribution BI-R-76-4.

SMITH, R.L. 1974. A description of current, wind and sea level variations during coastal upwelling off the Oregon coast, July-August 1972. *J. Geophys. Res.* **79**, no. 3: 435–43.

SMITH, S.D. and E.G. BANKE. 1975. Variation of the sea surface drag coefficient with wind speed. *Quart. J. Roy. Meteor. Soc.* **101**: 665–73.

THOMPSON, R. 1971. Topographic Rossby waves at a site north of the Gulf Stream. *Deep-Sea Res.* **18**: 1–20.

WARNER, J.L. 1970. Water movement on the Scotian Shelf. Ph.D. thesis, Dept of Oceanography, Dalhousie Univ., Halifax, N.S., 227 pp.

WORTHINGTON, L.F. 1964. Anomalous conditions in the slope water area in 1959. *J. Fish. Res. Board Can.* **21**, no. 2: 327–33.

Coastal Trapped Waves, with Application to the Northeast Pacific Ocean

D.G. Wright and L.A. Mysak*
Department of Mathematics, University of British Columbia, Vancouver, B.C.

[Manuscript received 6 January 1977; in revised form 2 May 1977]

ABSTRACT

The dispersion relation is derived for long coastal trapped waves of sub-inertial frequency that propagate along a single-step continental shelf in a two-layer fluid. When the internal (Rossby) deformation radius is smaller than the shelf width, we show that the dispersion relation can be factored exactly, giving two possible modes:

(i) an internal Kelvin wave modified by topography;

(ii) a continental shelf wave modified by the stratification.

A detailed discussion of the eigenfunctions associated with each of these modes is presented. Then the shelf wave dispersion relation is plotted for parameters applicable to the Oregon-Washington coast. Theoretical values for the periods and wavelengths predicted from these plots are shown to agree favorably with observed values for this region.

1 Introduction

Over the last decade increasing attention has been devoted to the study of coastal trapped waves: high frequency edgewaves, low frequency continental shelf waves and intermediate frequency Kelvin waves. (For a recent review of this topic, see LeBlond and Mysak (1977a)). In particular, there have been many recent studies dealing with the effects of on-shelf stratification on coastal trapped waves of sub-inertial frequency ($\omega < f$, where f = Coriolis parameter) (Kajiura, 1974; Allen, 1975; Wang, 1975; Wang and Mooers, 1976). For on-shelf stratification and under the rigid-lid approximation the trapped waves are shelf waves that are modified by the stratification or internal Kelvin waves that are modified by the topography. The purpose of this paper is to derive the dispersion relation for these two types of waves in the case of a single-step continental shelf in a two-layer fluid (see Fig. 1). The dispersion relation we derive fills a gap in the existing literature on coastal trapped waves. For example, Kajiura (1974) derived the dispersion relation for these waves only in the very low frequency limit ($\omega^2 \ll f^2$). Wang (1975), on the other hand, considered waves of higher frequencies ($\omega < f$), but gave no explicit form for

*Also Institute of Oceanography.

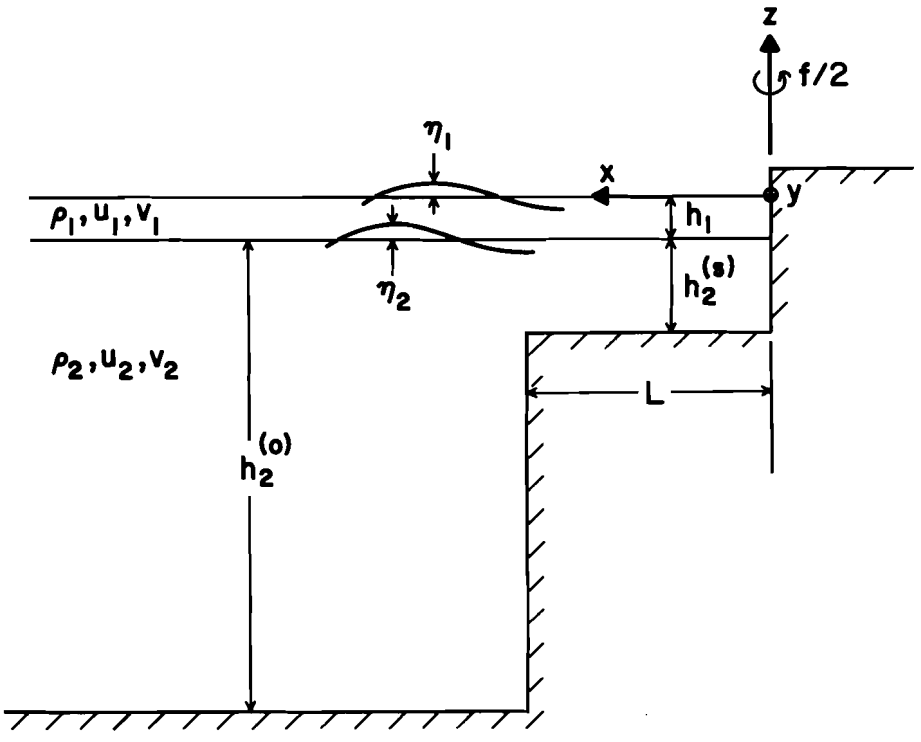

Fig. 1 Cross section of the two-layer model used in this paper. Coordinates x,y,z form a right-handed system which is rotating about the z axis with angular speed $f/2$.

the dispersion relation. In view of the relative simplicity and utility of this relation, we feel that it ought to be given further exposure in the literature.

The second purpose of this paper concerns the application of the dispersion relation to the shelf/slope waters off the Oregon-Washington coast where evidence of northward propagating (modified) shelf waves has been found by Huyer et al. (1975). A comparison of their observations with the theoretical results presented here is made; generally speaking, the agreement between the observations and the theory is quite good.

2 Basic equations for sub-inertial waves on a single-step shelf

We begin with the long-wave equations for an inviscid two-layer fluid rotating about the vertical with constant angular speed $f/2$:

$$u_{1t}^* - fv_1^* = -g\eta_{1x}^* \tag{1}$$

$$v_{1t}^* + fu_1^* = -g\eta_{1y}^* \tag{2}$$

$$(h_1u_1^*)_x + (h_1v_1^*)_y = \eta_{2t}^* \tag{3}$$

$$u_{2t}^* - fv_2^* = -g[\eta_1^* + \delta\eta_2^*]_x \tag{4}$$

$$v_{2t}^* + fu_2^* = -g[\eta_1^* + \delta\eta_2^*]_y \tag{5}$$

$$(h_2u_2^*)_x + (h_2v_2^*)_y = -\eta_{2t}^* \tag{6}$$

where: (u_1^*,v_1^*), (u_2^*,v_2^*) are the velocities in the upper and lower layers respectively; η_1^*,η_2^* are the surface and interfacial displacements; h_1,h_2 are the undisturbed depths of the upper and lower fluid layers which are taken as constant except for a step discontinuity in h_2 corresponding to the shelf break; g is the acceleration due to gravity and $0 < \delta = (\rho_2 - \rho_1)/\rho_2 \ll 1$. We note that terms of relative magnitude δ have been neglected in (4) and (5) (i.e. in each case $\eta_1^*(1 - \delta)$ has been approximated by η_1^*). Also, in (3) the rigid lid approximation has been made (i.e. $-\eta_{1t}^*$ on the right side of this equation has been neglected); this approximation requires that $f^2L^2/gh_1 \ll 1$, which guarantees that the neglected term, $-\eta_{1t}^*$, makes a negligible contribution to the vorticity balance. (For the Oregon-Washington coast, using the parameter values given in Section 5, we find that $f^2L^2/gh_1 = 49/650 \ll 1$). The rigid lid approximation eliminates all surface gravity waves and the external Kelvin wave from the system (LeBlond and Mysak, 1977b, Chapter 3).

Adding (3) and (6), we find that there exists a transport stream function ψ^* such that

$$\psi_x^* = -(h_1v_1^* + h_2v_2^*), \qquad \psi_y^* = (h_1u_1^* + h_2u_2^*). \tag{7}$$

Introducing complex amplitudes for each of the starred variables in the form $\zeta^*(x,y,t) = Re\{\zeta(x,y)\, e^{i\omega t}\}$, we now solve for u_1^*,v_1^* and u_2^*, v_2^* in terms of η_1^*,η_2^* from (1), (2) and (4), (5), respectively. Then combining these results with (7) gives

$$u_1 = \{\psi_y + ah_2(i\omega h_x + fh_y)\}/h_T \tag{8a}$$

$$u_2 = \{\psi_y - ah_1(i\omega h_x + fh_y)\}/h_T \tag{8b}$$

$$v_1 = \{-\psi_x + ah_2(i\omega h_y - fh_x)\}/h_T \tag{8c}$$

$$v_2 = \{-\psi_x - ah_1(i\omega h_y - fh_x)\}/h_T \tag{8d}$$

where $h \equiv \eta_2$, $a = g'/(f^2 - \omega^2)$, and $h_T = h_1 + h_2$. .

In contrast to the papers by Kajiura (1974) and Wang (1975), who worked with linear combinations of η_1 and η_2, we shall work with the variables ψ and h ($\equiv \eta_2$) (as does Allen (1975)). This approach facilitates comparison with the theories of barotropic shelf waves and internal Kelvin waves.

Cross-differentiating (1) and (2) and then using (3) gives

$$(h_1u_1)_y - (h_1v_1)_x = fh \tag{9}$$

provided $\omega \neq 0$; repeating the process using (4), (5) and (6) gives

$$(h_2u_2)_y - (h_2v_2)_x = -fh. \tag{10}$$

Finally adding (9) and (10) and using (7) we find

$$\psi_{xx} + \psi_{yy} = 0. \tag{11}$$

Subtracting $(1/h_2)$ times (10) from $(1/h_1)$ times (9) gives, after using (8):

$$h_{xx} + h_{yy} = \frac{1}{r^2} h, \tag{12}$$

where $r = [g'h_1h_2/(f^2 - \omega^2)h_T]^{1/2}$, which clearly reduces to the internal Rossby radius of deformation for $\omega^2 \ll f^2$.

3 Derivation of the dispersion relation for trapped waves

Since we are interested in trapped waves that propagate along the coast, we look for h and ψ in the form

$$h(x, y) = H(x)e^{i\ell y} \tag{13}$$

$$\psi(x, y) = \Psi(x)e^{i\ell y}. \tag{14}$$

We take $\ell > 0$ so that $\omega < 0$ (>0) corresponds to waves propagating in the positive (negative) y direction. From (11) and (12) we now have

$$\Psi_{xx} - \ell^2 \Psi = 0 \tag{15}$$

$$H_{xx} - \alpha^2 H = 0 \tag{16}$$

where $\alpha = [\ell^2 + (1/r)^2]^{1/2}$.

To distinguish variables on the shelf and in the deep ocean region we use the superscripts (o) (ocean) or (s) (shelf).

At $x = 0$ we require $u_1^{(s)} = u_2^{(s)} = 0$, which implies $\psi_y^{(s)} = 0$ and $i\omega h_x^{(s)} + f h_y^{(s)} = 0$. At the shelf break ($x = L$) we require continuity of the mass transport normal to the shelf in each layer, i.e.

$$\left.\begin{aligned} u_1^{(s)} &= u_1^{(o)} \\ h_2^{(s)} u_2^{(s)} &= h_2^{(o)} u_2^{(o)} \end{aligned}\right\} \text{ at } x = L. \qquad \begin{matrix} (17a) \\ (17b) \end{matrix}$$

Upon combining equations (17a,b) we may replace (17b) by:

$$\psi_y^{(s)} = \psi_y^{(o)} \text{ at } x = L. \tag{18}$$

We also require continuity of the interfacial and surface displacements at $x = L$, i.e.

$$\left.\begin{aligned} h^{(s)} &= h^{(o)} \\ i\omega v_1^{(s)} + f u_1^{(s)} &= i\omega v_1^{(o)} + f u_1^{(o)} \end{aligned}\right\} \text{ at } x = L. \qquad \begin{matrix} (19a) \\ (19b) \end{matrix}$$

(Equation (19b) is easily obtained from (2).) Finally the condition of trapping along the coast requires

$$\Psi^{(o)}, H^{(o)} \to 0 \text{ as } x \to \infty. \tag{20}$$

Applying the boundary conditions at $x = 0$ and at $x = \infty$, and then using (18) and (19a) we find:

$$\psi^{(s)} = A_1 \sinh(\ell x)e^{i\ell y} \tag{21}$$

$$\psi^{(o)} = A_1 \sinh(\ell L)e^{-\ell(x-L)}e^{i\ell y} \tag{22}$$

$$h^{(s)} = A_2[\omega\alpha^{(s)} \cosh(\alpha^{(s)}x) - f\ell \sinh(\alpha^{(s)}x)]e^{i\ell y} \tag{23}$$

$$h^{(0)} = A_2[\omega\alpha^{(s)} \cosh(\alpha^{(s)}L) - f\ell \sinh(\alpha^{(s)}L)]e^{-\alpha^{(0)}(x-L)}e^{i\ell y}. \tag{24}$$

Equation (17a) gives us the relation between A_1 and A_2, upon using (21) – (24) in (8a):

$$A_1 = -A_2 a\{\gamma^2 h_2^{(s)}(\omega^2\alpha^{(s)2} - f^2\ell^2)\sinh(\alpha^{(s)}L) \tag{25}$$
$$+ h_2^{(0)}(\omega\alpha^{(0)} - f\ell)(\omega\alpha^{(s)}\cosh(\alpha^{(s)}L) - f\ell \sinh(\alpha^{(s)}L))\}/(\gamma^2 - 1)\ell \sinh(\ell L)$$

where $\gamma^2 = h_T^{(0)}/h_T^{(s)}$ and a is as given earlier.

Finally, from (19b), the dispersion relation is found which after some rearrangement may be written as:

$$\{\gamma^2 h_2^{(s)}(\omega^2\alpha^{(s)2} - f^2\ell^2)T_1 + h_2^{(0)}(\omega\alpha^{(0)} - f\ell)(\omega\alpha^{(s)} - f\ell T_1)\}$$
$$\times \{\omega(T_2 + \gamma^2) + fT_2(1 - \gamma^2)\} = (1 - \gamma^2)\ell(f^2 - \omega^2) \tag{26}$$
$$\times (\omega\alpha^{(s)} - f\ell T_1)(\gamma^2 h_2^{(s)} - h_2^{(0)})T_2$$

where $T_1 = \tanh(\alpha^{(s)}L)$ and $T_2 = \tanh(\ell L)$.

4 Discussion of the dispersion relation

For $\omega^2 \ll f^2$, (26) reduces to a quadratic in ω so that the roots in this case are readily found for any range of parameter values. (See also Kajiura (1974; §4) for a discussion of the corresponding dispersion relation in the case of a free surface.) Another limit of particular interest is

$$\alpha^{(s)}L \equiv [\ell^2 + (f^2 - \omega^2)h_T^{(s)}/g'h_1h_2^{(s)}]^{1/2}L \gg 1 \tag{27}$$

so that $T_1 \simeq 1$. For $\omega^2 \ll f^2$ this will hold whenever the shelf width is much wider than the internal Rossby radius. As ω^2 approaches f^2 it is still quite possible for this limit to hold, since in general as ω/f increases so does ℓL (i.e. the longshore wavelength decreases). Clearly in any given case we need simply check that the approximation $T_1 \simeq 1$ is satisfied. Making the approximation $T_1 = 1$ in (26) we now have†

$$\omega\alpha^{(s)} = f\ell \text{ or}$$

$$\{\gamma^2 h_2^{(s)}(\omega\alpha^{(s)} + f\ell) + h_2^{(0)}(\omega\alpha^{(0)} - f\ell)\}\{\omega(T_2 + \gamma^2) + fT_2(1 - \gamma^2)\}$$
$$= (1 - \gamma^2)\ell(f^2 - \omega^2)(\gamma^2 h_2^{(s)} - h_2^{(0)})T_2. \tag{28}$$

The relation $\omega\alpha^{(s)} = f\ell$ may now be solved exactly to give $\omega/f = (r_i/L)\ell L$ or $\omega/f = 1$, where $r_i = [g'h_1h_2^{(s)}/f^2h_T^{(s)}]^{1/2}$ is the internal Rossby radius on the shelf. The first of these roots is the dispersion relation for an internal Kelvin wave on a very wide shelf (i.e. $L/r_i \gg 1$). We note here that for this root $\alpha^{(s)}L = (f/\omega)\ell L = L/r_i$ so that whenever the shelf is wide compared to the internal Rossby radius, the internal Kelvin wave is unaffected by the finiteness of the shelf width (i.e. the Kelvin wave and shelf wave uncouple). The second root is apparently an inertial oscillation; however an analysis of the primitive equations (1) – (6) shows that for the case of a rigid upper surface no motion

†This limiting case was noted by Wang (1975) but the relation (28) was not explicitly given.

is possible at the inertial frequency in the presence of the assumed topography. The origin of this spurious root is the assumption throughout the paper that $\omega \neq f$ so that we could freely manipulate terms involving $\omega^2 - f^2$. For example in the derivation of (12) we multiplied each side by $\omega^2 - f^2$.

The remaining roots are given by $\omega = 0$ and

$$\frac{\omega}{f} = -\frac{\ell(h_2^{(s)}\gamma^2 - h_2^{(0)})(T_2 + \gamma^2) + (\gamma^2\alpha^{(s)}h_2^{(s)} + \alpha^{(0)}h_2^{(0)})T_2(1 - \gamma^2)}{(\gamma^2\alpha^{(s)}h_2^{(s)} + \alpha^{(0)}h_2^{(0)})(T_2 + \gamma^2) + \ell(h_2^{(s)}\gamma^2 - h_2^{(0)})T_2(1 - \gamma^2)}. \quad (29)$$

As we have assumed a priori that $\omega \neq 0$ (see (9)), the first root is spurious. The second root (29) is the continental shelf wave as modified by density stratification. The case of a shelf wave in a homogeneous fluid with a rigid lid is readily obtained from (29) by taking the limit $h_1 \to 0$. In this case $\alpha^{(s)}/\ell$, $\alpha^{(0)}/\ell \to \infty$ and we have

$$\omega/f = (\gamma^2 - 1)\tanh(\ell L)/[\gamma^2 + \tanh(\ell L)],$$

in agreement with Larsen (1969).

It is interesting to note further that in the limit $\omega^2 \ll f^2$, the right-hand side of (29) is independent of ω and hence we have a relatively simple formula for ω/f. If $\omega/f \sim O(1)$, (29) may be solved by simple linear iteration using the limiting solution ($\omega^2 \ll f^2$) as the initial approximation.

5 Discussion of the eigenfunctions

It is interesting at this point to examine the velocity distributions as a function of x corresponding to the Kelvin and shelf-wave modes found above. Substituting equations (21) – (24) into (8) and choosing the arbitrary constant A_2 to be real (which may be arranged by choosing the initial time appropriately), we find the following expressions for the velocity components:

$$u_{1,2}^{(s)} = -A_2\{(A_1/A_2)\ell \sinh(\ell x) \pm ah_{2,1}^{(s)} \sinh(\alpha^{(s)}x) \times (\omega^2\alpha^{(s)2} - f^2\ell^2)\} \sin(\ell y + \omega t)/h_T^{(s)}$$

$$v_{1,2}^{(s)} = A_2\{-(A_1/A_2)\ell \cosh(\ell x) \pm ah_{2,1}^{(s)}[\cosh(\alpha^{(s)}x)\ell\alpha^{(s)}(f^2 - \omega^2) - \sinh(\alpha^{(s)}x)\omega f(\alpha^{(s)2} - \ell^2)]\} \cos(\ell y + \omega t)/h_T^{(s)}$$

$$u_{1,2}^{(0)} = -A_2\{(A_1/A_2)\ell \sinh(\ell L)\exp[-\ell(x - L)] \pm ah_{2,1}^{(0)}[\omega\alpha^{(s)}\cosh(\alpha^{(s)}L) - f\ell \sinh(\alpha^{(s)}L)](f\ell - \omega\alpha^{(0)})\exp[-\alpha^{(0)}(x - L)]\} \sin(\ell y + \omega t)/h_T^{(0)}$$

$$v_{1,2}^{(0)} = A_2\{(A_1/A_2)\ell \sinh(\ell L)\exp[-\ell(x - L)] \pm ah_{2,1}^{(0)}[\omega\alpha^{(s)}\cosh(\alpha^{(s)}L) - f\ell \sinh(\alpha^{(s)}L)](f\alpha^{(0)} - \omega\ell)\exp[-\alpha^{(0)}(x - L)]\} \cos(\ell y + \omega t)/h_T^{(0)}$$

where the upper sign in each case corresponds to the first subscript and the lower sign to the second. A_1/A_2 is given by (25).

We will refer to the complete factor multiplying the trigonometric function as the amplitude of the velocity component. Let us now consider the amplitudes of the two modes. For the purpose of calculation we shall work with the case $\ell L = 0.3$ and choose all the other parameters as appropriate to the Oregon-Washington coast (see Section 6).

(i) The internal Kelvin wave (Fig. 2): Since this wave is trapped on the shelf and decays exponentially away from $x = 0$ on the scale of the internal (Rossby) deformation radius, we have normalized the amplitudes with respect to the amplitude of $v_1^{(s)}$ at $x = 0$. The velocity component normal to the coast vanishes identically and the longshore velocities in the upper and lower layers, being baroclinic, are in the ratio $-h_2/h_1$. Since $\alpha^{(s)}L \gg 1$, the motion is confined to the shelf region.

(ii) The (modified) shelf wave (Fig. 3): In this figure the velocities are normalized with respect to $v_1^{(s)}$ $(x = L)$. The velocity in the upper layer is continuous across the shelf break while in the lower layer it is, of course, discontinuous. We note that except near the shelf break, the motion is barotropic (or nearly so) and decays away from the shelf on the scale of the longshore wavelength of the motion. When the longshore wavelength is increased, the only significant change is that the velocity component normal to the coast is decreased to account for the change in relative scales for offshore and longshore directions.

In the next section we will show that the observations made by Huyer et al. (1975) along the Oregon-Washington coast are consistent with the idea of a modified shelf wave propagating northward along the shelf.

6 Application to the Oregon-Washington coast

To apply our single-step shelf model to the northwest coast of North America we take the following parameter values: $f = 10^{-4}$ s^{-1}, $g' = 0.02$ m s^{-2}, $L = 70$ km, $h_1 = 65$ m, $h_T^{(s)} = 200$ m, $h_T^{(o)} = 3000$ m, for which $f^2L^2/gh_1 \simeq 49/650$ and hence the rigid lid approximation made in Section 2 is valid. It was found from numerical tests that these values may be varied considerably without seriously affecting the numerical value of the modified shelf-wave root. Of particular interest is the insensitivity of this root to variations in the upper layer depth h_1. This accounts for the success of the barotropic shelf-wave theory in cases where one might think the on-shelf stratification would be important. Wang (1975) has also noted that at low frequencies the shelf wave is affected very little by the stratification. The dispersion relation (29) corresponding to the above parameter values is plotted in Figure 4. (For the above parameter values, $r_i/L \simeq 0.12$ and hence (29) is valid at least for $\omega^2 \ll f^2$.) For comparison, the internal Kelvin wave dispersion relation for the same parameter values is also shown in this figure. The approximation $T_1 = 1$ is in fact satisfied to within 0.05% for all ℓL. The horizontal lines crossing the shelf-wave curve in Fig. 4 are derived from recent observations reported by Huyer et al. (1975). They found that the current, sea level and wind spectra on the Oregon-Washington shelf were peaked at $\omega/f = 0.11$, 0.2 and 0.29 (corresponding to 0.16, 0.3 and 0.44 cpd). At each of these frequencies the phase lags between successive stations were also estimated. From the phase lag between two stations at a given frequency and the distance between the stations, the wavelength was determined. The horizontal bars in Fig. 4 represent the 95% confidence limits for these observed wavelengths at the peak frequencies

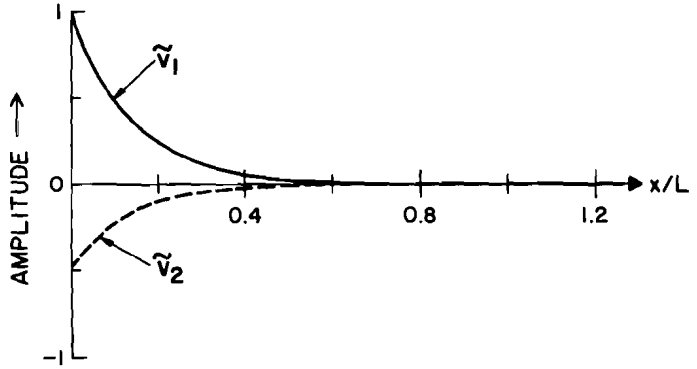

Fig. 2 The velocity amplitude for the internal Kelvin wave normalized with respect to $v_1^{(s)}$ $(x = 0)$. The values of the parameters used are given in Section 6; $\ell L = 0.3$ (wavelength = 1466 km).

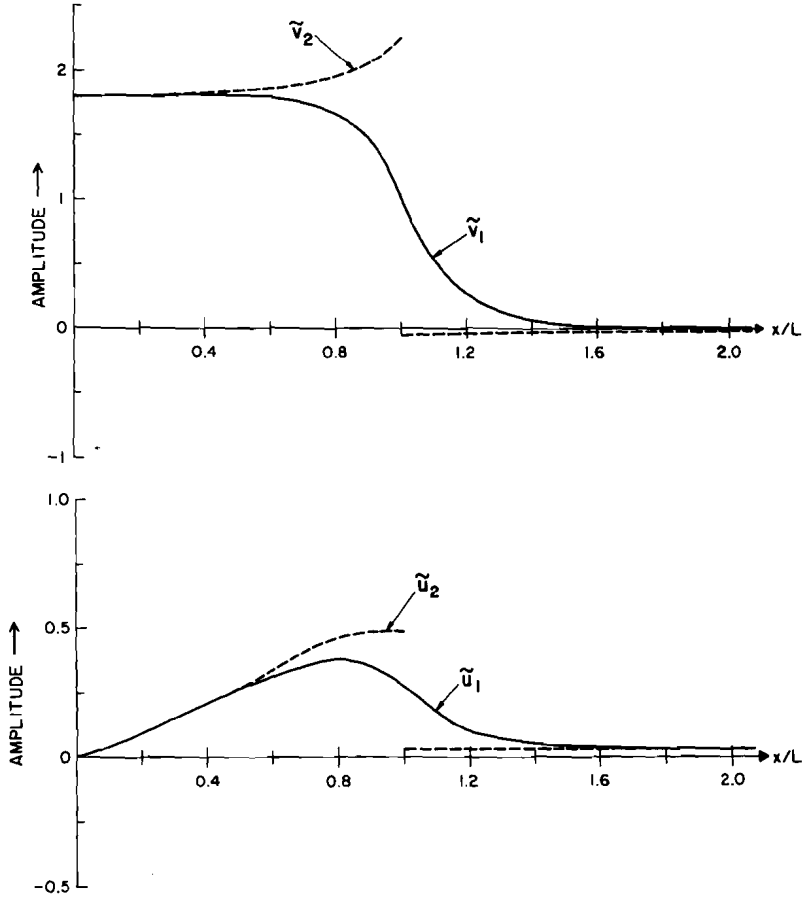

Fig. 3 The velocity amplitudes for the modified shelf wave normalized with respect to $v_1^{(s)}$ $(x = L)$. The values of the parameters used are given in Section 6; $\ell L = 0.3$ (wavelength = 1466 km).

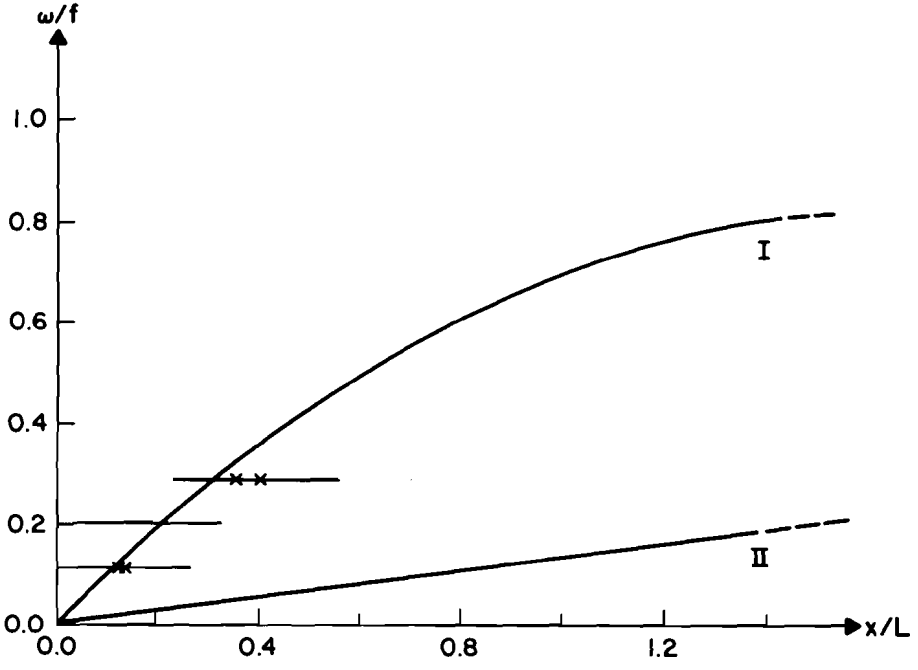

Fig. 4 The shelf wave (I) and internal Kelvin wave (II) dispersion relations for the Oregon-Washington coast. The horizontal lines represent the 95% confidence limits for the wavelengths of low-frequency, northward-moving waves observed by Huyer et al. (1975). The segment marked by crosses at the frequency $\omega/f = 0.11$ is the wavelength interval common for all observed current, wind and sea-level pairs, while that at $\omega/f = 0.29$ is the wavelength interval common to the current and sea-level observations only.

given above. The segment marked by crosses at the frequency $\omega/f = 0.11$ is the wavelength interval common for all current, wind and sea-level pairs. At $\omega/f = 0.29$ the wavelength interval common to current and sea level is marked. The wind does not have a wavelength interval common with the current and sea level at this frequency. The relatively large wavelength interval at $\omega/f = 0.2$ is due to low coherence in the signal at that frequency. Clearly the shelf-wave results for our step-shelf model agree well with the observations. As mentioned earlier the simple barotropic shelf-wave model also agrees well with the observations of Huyer et al. (1975) (differing from the two-layer model by less than 3.5% even at $\ell L = 5$).† As expected, the results from the barotropic theory do give slightly lower values for ω/f but the agreement even for $\omega/f = O(1)$ is rather surprising (at $\ell L = 5$, $(\omega/f)^2 \simeq 0.8$).

At this point it is interesting to compare the baroclinicity of the currents predicted by our model with the observations made by Huyer et al. (1975). They found that vertical phase differences were essentially zero and the current

†This is rather an important result since the introduction of two-layer *deep-sea* stratification typically increases the speed of a barotropic shelf wave by a factor of two (Mysak, 1967; Kajiura, 1974).

amplitudes were depth-independent (i.e. the motions were barotropic) wherever the coherence was high and phase estimates most reliable. This is consistent with the predictions made from our simple model except within a couple of Rossby radii of the shelf break where the currents are expected to be bottom trapped (see Fig. 3). However, little weight should be given to the theoretical predictions made near the depth discontinuity, since in reality such a sharp break in the shelf rarely occurs.

Finally, we note that a shelf wave propagating northward along the Oregon-Washington coast must pass Juan de Fuca Strait, and in so doing may excite low frequency motions in the Strait. Indeed, while examining the possibility of using pressure measurements to determine the currents flowing through the Strait, Fissel (1976) observed that about 80% of the total variance of the residual currents‡ occurred at frequencies less than 0.2 cpd. Work is now in progress to determine whether this low frequency energy is related to the shelf-wave energy off the Oregon-Washington coast.

Acknowledgements

This paper was written while D.G.W. was supported by a postgraduate National Research Council of Canada Scholarship and a UBC Mathematics Department Teaching Assistantship. The support of the National Research Council of Canada through operating grant A5201 to L.A.M. is also gratefully acknowledged. The authors are also indebted to the referees for their helpful comments.

References

ALLEN, J.S. 1975. Coastal trapped waves in a stratified ocean. *J. Phys. Oceanogr.* **5**, 300–325.

FISSEL, D.E. 1976. Pressure differences as a measure of currents in Juan de Fuca Strait. Pacific Marine Science Report 76–17, Institute of Ocean Sciences, Patricia Bay, Victoria, B.C. (unpublished manuscript), 63 pp.

HUYER, A.; B.M. HICKEY; J.D. SMITH; R.L. SMITH; and R.A. PILLSBURY. 1975. Alongshore coherence at low frequency in currents observed over the continental shelf off Oregon and Washington. *J. Geophys. Res.* **80**, 3495–3505.

KAJIURA, K. 1974. Effect of stratification on long period trapped waves on the shelf. *J. Oceanogr. Soc. Japan*, **30**, 271–281.

LARSEN, J.C. 1969. Long waves along a single step topography in a semi-infinite uniformly rotating ocean. *J. Marine Res.*, **27**, 1–6.

LE BLOND, P.H. and L.A. MYSAK. 1977a. Trapped coastal waves and their role in shelf dynamics. In *The Sea*, Vol. 6, (edited by E.D. Goldberg, I.N. McCave, J.J. O'Brien and J.M. Steele), Wiley-Interscience, New York, pp. 459–495.

——— and ———. 1977b. *Waves in the Ocean.* Elsevier, Amsterdam, in press.

MYSAK, L.A. 1967. On the theory of continental shelf waves. *J. Marine Res.*, **25**, 205–227.

WANG, D. 1975. Coastal trapped waves in a baroclinic ocean. *J. Phys. Oceanogr.* **5**, 326–333.

——— and C.N.K. MOOERS. 1976. Coastal-trapped waves in a continuously stratified ocean. *J. Phys. Oceanogr.* **6**, 853–863.

‡Residual currents are defined as the remainder of the currents after removing variations with frequencies above 0.8 cpd.

The Energy of Near-Surface Internal Waves in the Strait of Georgia

G. Samuels and P.H. LeBlond
Institute of Oceanography
University of British Columbia
Vancouver, B.C.

[Manuscript received 17 September 1976; in revised form 14 June 1977]

ABSTRACT
An estimate of the energy content of near-surface internal waves in the Strait of Georgia is obtained from a combination of aerial photographs and *in-situ* measurements. The role of these waves in the tidal energy budget and in the mixing processes in the Strait is discussed.

1 Introduction

High-frequency internal gravity waves (of periods ranging from one to thirty minutes) are commonly observed in many coastal areas of the oceans. Such areas are usually endowed with a strong near-surface pycnocline so that interfacial waves are visible from the air through their surface manifestations, either through slick formation (Ewing, 1950), interactions with short surface waves (Gargett and Hughes, 1972), or variations in the colour of the sea-surface. Groups of such waves have been observed in many locations (Shand, 1953; Curtin and Mooers, 1975) and in some cases are even detectable from satellite photographs (Apel et al., 1975). Because of the visibility of near-surface internal waves, the area of sea surface over which they occur may be determined from aerial photographs. With the help of some representative "ground truth", it should then be possible to estimate the energy content of these waves. This method is complementary to the usual measurements of internal wave energy, based on single point moorings or horizontal transects; in many coastal regions, where the internal wave field is spatially inhomogeneous, information on the horizontal distribution of the waves may be necessary to obtain an estimate of their energy content. Furthermore, the grouping of the observed wave trains suggests generation by scattering of the barotropic tide over bathymetric features such as the edge of the continental shelf or abrupt ridges. An estimate of the energy density of interfacial waves would throw light on their relevance to tidal energy dissipation in coastal areas.

The Strait of Georgia lends itself rather well to an energy budget of high-frequency internal waves. Because of the sharp density stratification near the surface due to the large outflow of fresh water from the Fraser river (especially during summer freshet; cf. Waldichuk, 1957), internal wave activity is concentrated near the surface and is readily detected from the air (see, for example, Fig. 1). Geometrical constrictions, such as at Boundary Pass (Fig. 2),

Fig. 1 Aerial photograph of internal waves in the southern Strait of Georgia. Photo taken on May 29, 1968, from an altitude of ≃750 m. The camera points eastward and the distance between the first two bands in the wave group is about 100 m.

where the waves are observed to be generated are easily identified, and the tidal energy flux and dissipation through these constrictions may be estimated from available data.

2 Data

The data on internal wave coverage of the southern Strait of Georgia were gathered on a clear day (May 29, 1968) during a series of six flights over the

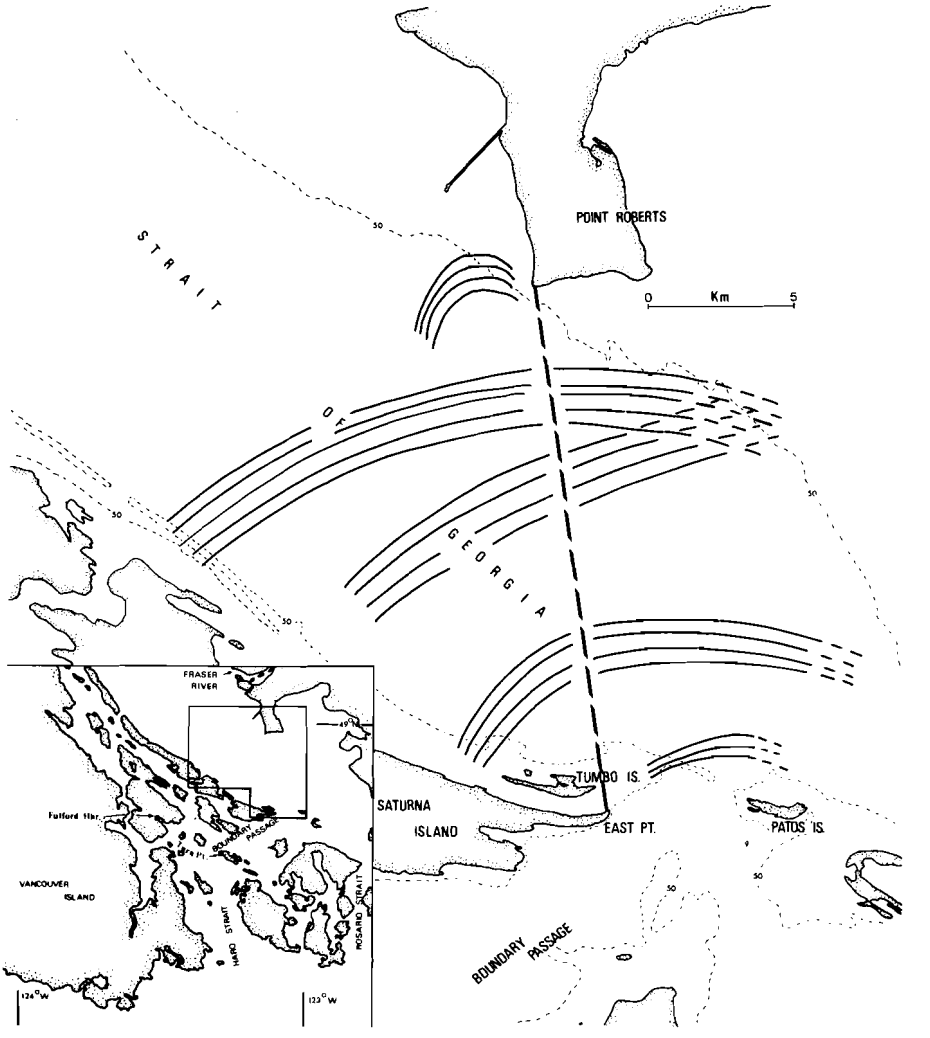

Fig. 2 Internal wave groups in the Southern Strait of Georgia. The lines drawn delineate the areas of the wave groups (but not individual wave fronts) during one of the flights of May 29, 1968. The eastern extension of the wave groups could not be determined precisely and has been shown by broken lines. The flight line between Point Roberts and East Point, along which the photographs were taken, is also shown. The 50-fathom depth contour is shown as a dotted line; note the presence of the sill at the northern end of Boundary Passage.

area. These flights, at an altitude of 2,500 ft (762 m), were taken on a line joining the southwest tip of Point Roberts and East Point on Saturna Island (Fig. 2). The time of passage over these landmarks was clocked in both directions, and photographs of the most prominent visible internal wave groups were taken at measured times. It was then possible to calculate the position

at which every photograph was taken and to construct sketches of the internal wave trains in the area covered (Fig. 2). During the four afternoon flights over which the best photographs were obtained, there was no difficulty in determining the westward extension of the internal wave groups from the line of flight: in that direction, the internal waves manifested themselves by variations in the amplitude of the direct specular reflection of sunlight. Towards the east, however (such as in Fig. 1), the waves were detected by variation in the intensity of the reflected skylight and the eastern extension of the wave groups could not be ascertained with precision. The estimates quoted below for the area covered by internal waves should not be in error by more than about 50% on this account.

3 Analysis and discussion

In order to calculate the energy of the observed wave groups, the density stratification and the wave amplitudes need to be known. The summer density stratification in the Strait of Georgia is strongest near the mouth of the Fraser River (Waldichuk, 1957) and decreases toward the southern passes, where the internal waves are generated (Gargett, 1976). Observations taken on the day following the flights (30 May, 1968) by Crean and Ages (1971) show that the relative contrast between the density ρ_2 at a depth of 10 m and that of the surface water ρ_1, defined as $(\rho_2 - \rho_1)/\rho_2$, varies from 0.015 near the Fraser River mouth to 0.007 near Boundary Passage. The energy estimates have been performed by assuming that the density contrast varied linearly with position between these extreme values and by using a uniform upper layer depth $h_1 = 10$ m. No direct measurements of internal wave amplitudes were performed at the time of the flights. Observations under similar circumstances (Hughes, 1969; Gargett, 1976) have shown that isotherm displacements of up to 6 m are common. The measurements of Gargett (1976) were performed at a position almost due north from East Point at the location of the second wave group from Boundary Pass shown in Fig. 2. As the waves spread radially and slowly dissipate while propagating away from their source their amplitudes should decrease northwestwards from Boundary Passage.

The energy density per unit area of interfacial waves of amplitude a may be written

$$E = \tfrac{1}{2}(\rho_2 - \rho_1) g a^2 F\left(\frac{a}{h_1}, \ldots\right) \tag{1}$$

where F is a function of the wave amplitude (a/h_1) and of other non-dimensional parameters, such as the actual shape of the density transition. For the rough estimate performed in this note, the factor F has been taken as unity, corresponding to small amplitude waves. Even though the linear approximation $F = 1$ is clearly invalid over much of the internal wave field (considering the wave amplitudes quoted above), it is believed that by taking a sufficiently large range of wave amplitudes the energy estimates should encompass the effects of non-linearity. The total area of the wave groups was measured from

TABLE 1. Estimated energies and areas of the observed internal wave fields. From the salinity and temperature data of Waldichuk (1957), a range of possible density contrasts straddling the observations by Crean and Ages (1971) was estimated for the day following that when the photographs were taken. Estimates of wave amplitudes from Hughes (1969) and Gargett (1976) were also used, ranging from the full thickness of the upper layer to one half of that thickness. The minimum, maximum and mean values of all possible choices are listed, together with their averages for the four flights

Flight	Energy (J)			Observed area (m^2)
	Minimum	Maximum	Mean	
1	1.2×10^9	9.3×10^9	4.5×10^9	5.9×10^7
2	1.6×10^9	9.4×10^9	4.8×10^9	7.6×10^7
3	2.0×10^9	1.3×10^{10}	6.5×10^9	1.1×10^8
4	1.6×10^9	1.1×10^{10}	5.8×10^9	9.3×10^7
Average	1.6×10^9	1.1×10^{10}	5.4×10^9	8.5×10^7

sketches similar to that shown in Fig. 2, and the energy of the wave groups was computed for a range of possible wave amplitudes (Table 1). The calculations were performed for four afternoon flights and were similar for each flight. The horizontal energy density computed for near-surface internal waves is of the order of $E = 10^2$ J m^{-2}. This value is considerably smaller than that ($E_{GM} = 4 \times 10^3$ J m^{-2}) found by Garrett and Munk (1972) to provide the best fit to oceanic internal wave spectra. This discrepancy should not be too surprising, since the Garrett-Munk energy density covers a broad frequency band (from the inertial frequency to the Brunt-Väisälä frequency), whereas the interfacial waves observed in the Strait of Georgia all lie in a rather narrow band of high frequencies (with periods ranging approximately from 10 s to 5 min).

Observations (cf. Gargett, 1976) indicate that the high-frequency interfacial waves detected by aerial photography in the Strait of Georgia are generated mainly by topographic scattering of the flood tide over the sill lying between East Point (on Saturna Is.) and Patos Is., at the northern end of Boundary Passage (Fig. 2). The sea-level variation and the tidal current in Boundary Passage are shown in Fig. 3 for a period covering that over which the photographs were taken. The sea level is actually that obtained from the Canadian Hydrographic Service Tide Tables for 1968 at Fulford Harbour. From the results of Crean (1976), the phase and the amplitude of tidal sea-level displacements are the same at East Point as at Fulford Harbour. The currents shown in Fig. 3 are scaled up (to a maximum flood of 3 knots) and delayed (by 30 min) from those given by the same Tide Tables for Turn Point, according to the instructions given in those tables. Note that the maximum flood current at East Point (at 1800 PST, May 29) leads the surface elevation (high tide at 2035, May 29) by about 2½ hours. Since the tide is dominated by the semidiurnal component M2, this time lag corresponds to a phase lag

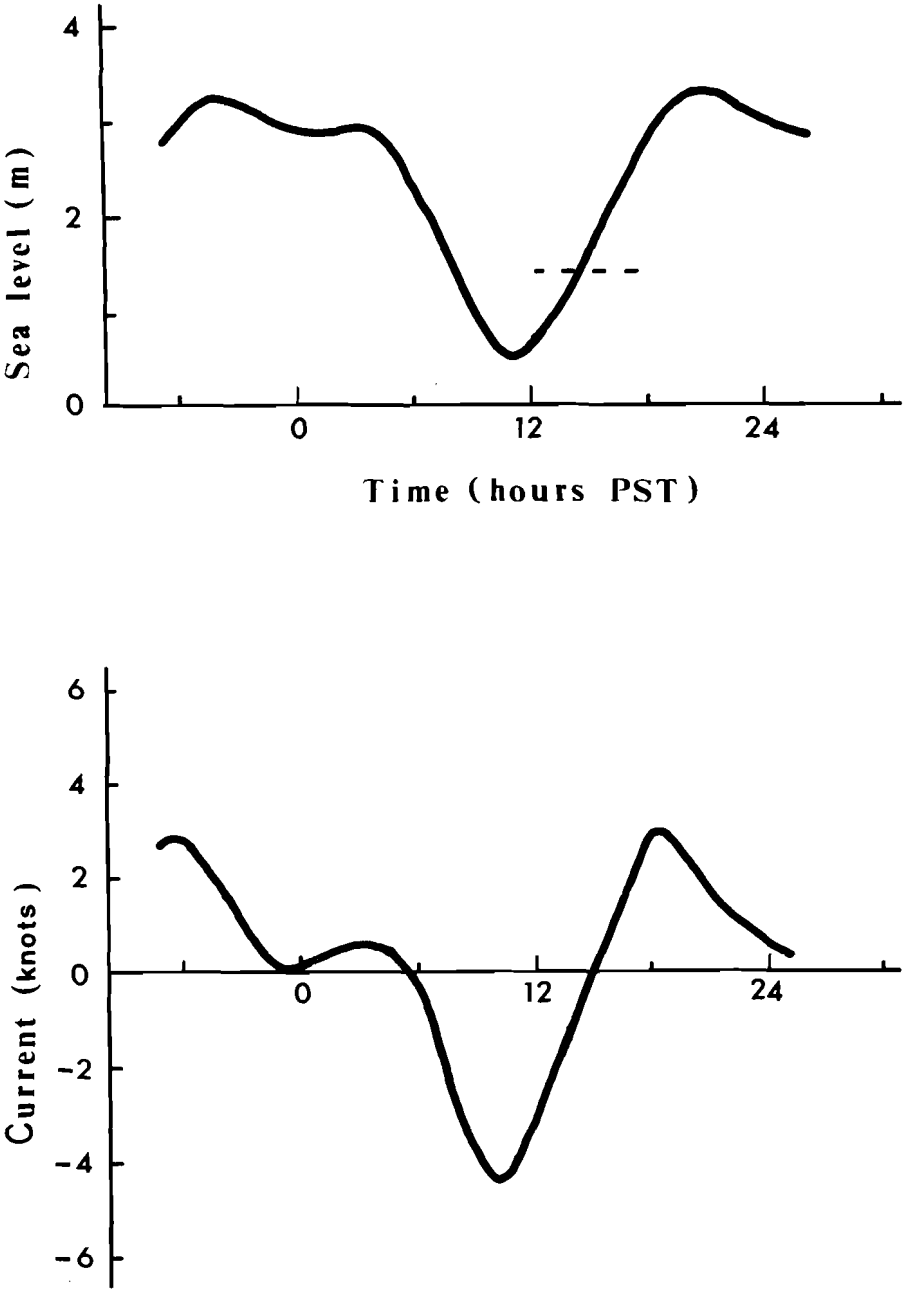

Fig. 3 Sea-level variation (above) and currents (below) at East Point on May 29, 1968 (from Canadian Hydrographic Service Tide Tables). Flood currents, into the Strait of Georgia from Boundary Passage, are taken as positive. The times of the four flights mentioned in the text (1223–1248; 1352–1423; 1539–1604; 1707–1729 PST) are indicated on the sea level graph. (1 knot = 0.51 m s^{-1}.)

of about 72°. Although some of the internal wave groups could be clearly observed to have been generated during the flood starting at about 1445 PST, May 29, it was not possible to positively identify wave groups on successive photographs so as to trace their individual progress away from their source. Using an estimate of the speed of travel of the internal waves, we have assumed that the wave groups seen in the area of observation were all generated within one flood period (about 6 h).

The approximate group velocity for waves travelling at the interface between a thin upper layer and a deep lower layer, and with wavelengths in excess of the thickness h_1 of the upper layer, is given by

$$C_g = \sqrt{\frac{g(\rho_2 - \rho_1)h_1}{\rho_2}}. \tag{2}$$

With a mean density contrast $(\rho_2 - \rho_1)/\rho_2 = 10^{-2}$ and $h_1 = 10^{-2}$, $C_g = 1.0$ m s^{-1} (2 knots). Adding to this a mean flood current of the order of about one half knot (Crean, pers. comm.) in the southern Strait of Georgia, we find that an internal wave group can travel away from its generation area in Boundary Passage a distance of about 15 nautical miles (25 km) in a six-hour flood. This distance is quite sufficient to cover the area of observations.

Let us now compare the energy contained in the internal wave field radiated from the mouth of Boundary Passage to that lost by the tide in the area of generation. In his model of the barotropic tides in the Strait of Georgia, Crean (1976) finds that most of the energy dissipation occurs in the narrow passages (Haro Strait and Rosario Strait) connecting the Strait of Georgia proper to the Strait of Juan de Fuca. On the basis of a bottom frictional force of the form $\rho k\,\mathbf{u}|\mathbf{u}|/h$ commonly used in tidal models (Dronkers, 1964), where k is a friction coefficient, $\mathbf{u}$ the depth-averaged horizontal velocity vector and h the depth, the rate of energy dissipation per unit volume is equal to $\rho k|\mathbf{u}|^3/h$. With an alternating rectilinear tidal current of the form $u = U_0 \sin \omega t$, the total dissipation per unit volume over half a tidal cycle (the flood) becomes

$$D/\text{volume} = \int_0^{T/2} \frac{\rho k U_0^3}{h} |\sin^3 \omega t| dt = \frac{4}{3} \frac{U_0^3 \rho k}{\omega h}. \tag{3}$$

Since the internal waves are observed to be generated during the flood tide through Boundary Passage, it is appropriate to compare their energy content to the total dissipation during that time in the generation area, over the sill lying between East Point and Patos Is. This sill is taken as having a mean depth of 60 m, a width of about 500 m and a cross-channel length of about 4 km. Taking $U_0 = 1.5$ m s^{-1} (3 knots) and the frequency ω as that of the dominant semidiurnal tide ($\omega \simeq 1.4 \times 10^{-4}$ s^{-1}), together with the large value of the friction coefficient ($k = 0.03$) which Crean (pers. comm.) found necessary to use in Haro Strait to calibrate his tidal model, we found that the energy dissipated by tidal friction over the generating ridge is

$$D = 1.9 \times 10^{12} \text{ J},$$

a value which exceeds the maximum internal wave energy estimate of Table 1 by two orders of magnitude. Thus, in spite of the uncertainties associated with the method of comparison, it appears that even in the very area of generation the amount of energy radiated as internal waves is greatly inferior to that dissipated by the barotropic tide. *A fortiori*, the transfer of energy into internal waves is an insignificant fraction of the total energy dissipation in the whole of the Strait of Georgia.

It is also of interest to estimate the role of high-frequency internal waves in mixing the upper and lower layers and in thus eroding the density stratification. Assuming, as an extreme situation, that while travelling from Boundary Passage to the Fraser River area an internal wave train loses all its energy by mixing at the density discontinuity, thus increasing the potential energy density of the water column, the average deepening of the surface layer may be derived quite simply.

Assuming mass conservation, the mixing of upper layer water (of thickness h_1 and density ρ_1) with deeper water of density ρ_2 produces an upper layer thicker than h_1 by an increment Δh and of density ρ_3 given by

$$\rho_3 = (h_1\rho_1 + \Delta h\rho_2)/(h_1 + \Delta h). \tag{4}$$

The increase in potential energy of gravitation (referred to a depth $z = -h_1 - \Delta h$) per unit area of the sea surface upon mixing is then given by

$$\Delta E = g\Delta h(\rho_2 - \rho_1)h_1/2. \tag{5}$$

With a mean density contrast $(\rho_2 - \rho_1) = 10$ kg m^{-3}, $h_1 = 10$ m, and $\Delta E \simeq 10^2$ J m^{-2}, $\Delta h \simeq 20$ cm. However, laboratory experiments by Thorpe (1973) indicate that only about 5% of the turbulent energy dissipated by breaking internal waves finds its way into gravitational potential energy of stratification. The mean deepening Δh must then be reduced to about 1 cm. The upper layer is so thin that a minimum of wind action (Denman, 1973) will easily mask any effects due to internal wave mixing, the deepening due to mixing being in any case beyond the limits of practical measurement accuracy.

4 Conclusion

In spite of their spectacular and ubiquitous nature, it appears that the high-frequency near-surface internal waves observed in the Strait of Georgia play an insignificant role in the energy balance of the local waters. This result should also apply to other similar coastal areas.

References

APEL, J.R.; H.M. BYRNE; J.R. PRONI; and R.L. CHARNELL. 1975. Observations of oceanic internal and surface waves from the Earth Resources Technology Satellite. *J. Geophys. Res.* **80**: 865–881.

CREAN, P.B. 1976. Numerical model studies of the tide between Vancouver Island and the mainland coast. *J. Fish. Res. Board Can.* **33**: 2340–2344.

——— and A.B. AGES. 1971. Oceanographic records from 12 cruises in the Strait of Georgia and Juan de Fuca

Strait, 1968, Vol. 3, Spring. Dept. Energy, Mines and Resources, Marine Sciences Branch, Victoria.

CURTIN, T.B. and C.N.K. MOOERS. 1975. Observation and interpretation of a high frequency internal wave packet and surface slick pattern. *J. Geophys. Res.* **80**: 872–894.

DENMAN, K.L. 1973. A time-dependent model of the upper ocean. *J. Phys. Oceanogr.* **3**: 173–184.

DRONKERS, J.J. 1964. *Tidal computations in rivers and coastal waters.* North Holland Publishers, Amsterdam. 518 pp.

EWING, M. 1950. Slicks, surface films and internal waves. *J. Marine Res.* **9**: 161–187.

GARGETT, A.E. 1976. Generation of internal waves in the Strait of Georgia, British Columbia. *Deep-Sea Res.* **23**: 17–32.

——— and B.A. HUGHES. 1972. On the interaction of surface and internal waves. *J. Fluid Mech.* **52**: 179–191.

GARRETT, C.J.R. and W. MUNK. 1972. Space-time scales of internal waves. *Geophys. Fluid Dynamics.* **2**: 225–264.

HUGHES, B.A. 1969. Characteristics of some internal waves in Georgia Strait. Tech. Memo. 69–2. Defence Res. Estab. Pacific, Victoria, 23 pp.

SHAND, J.A. 1953. Internal waves in Georgia Strait. *Trans. Amer. Geophys. Union*, **34**: 849–856.

THORPE, S.A. 1973. Turbulence in stably stratified fluids: a review of laboratory experiments. *Boundary-Layer Meteorol.* **5**: 95–119.

WALDICHUK, M. 1957. Physical oceanography of the Strait of Georgia, British Columbia. *J. Fish. Res. Board Can.* **14**: 321–486.

BOOK REVIEW

ADVANCES IN GEOPHYSICS, volumes 18A and 18B. Turbulent diffusion in environmental pollution. F.N. Frenkiel and R.E. Munn, editors. Academic Press, New York, 1974, 861 pp, hardcover, $28.50 each.

Meteorologists and oceanographers studying the dispersion of pollution will be keenly interested in volumes 18A and 18B of *Advances in Geophysics* which are devoted solely to the proceedings of an International Symposium on Turbulent Diffusion in Environmental Pollution, held in Charlottesville, Virginia, in April 1973. This review is meant to give some insight into what the reviewer feels is a very comprehensive state-of-the-art report (as of 1973) in the turbulent diffusion of pollution.

The two editors, F.M. Frenkiel of the U.S.A. and R.E. Munn of Canada, have arranged the sixty-two papers more or less in the order in which they were given at the Symposium. Consequently, papers are grouped by topic, although there is no indication of this. A list of papers by session is, however, conveniently given at the end of volume 18B. The papers cover a very wide range of topics in environmental diffusion, including fundamentals of diffusion, the behaviour of the planetary boundary layer, global and regional scale dispersion, mathematical and physical modelling of diffusion, and sink mechanisms for atmospheric pollutants. The great majority of the papers deal with atmospheric pollution, but there is also a group dealing with oceanic pollution. Volume 18A tends to stress the theoretical aspects of diffusion; Volume 18B, the applied.

Volume 18A leads off with a history by J. Kampé de Fériet of the first twenty-five years of the study of turbulent diffusion including the works of Boussinesq, Reynolds, Fick, and Taylor. This paper provides a convenient review for someone who has not examined the background concepts for some time. The next paper by S. Corrsin is a severe critique of the gradient theory equations so dear to the hearts of many applied meteorologists and engineers. Corrsin examines the necessary (but not sufficient) conditions for the validity of gradient transport models and concludes that their partial success (which no doubt results in their great popularity) is "largely fortuitous and certainly surprising." Corrsin suggests that corrective terms be added to gradient models while basic research proceeds to formulate a fundamentally more correct model which can be used practically. It is fortunate that Corrsin's paper appears near the beginning of the proceedings; it seems meant to shake the complacency of those of us who tend to forget about the complexity of turbulent diffusion.

The next group of papers deals with the boundary layer next to the earth's surface, with emphasis on the prediction of the height of the boundary layer both stably stratified (paper by J.A. Businger and S.P.S. Arya) and convectively unstable (paper by D.J. Carson and F.B. Smith). The latter problem has great practical importance because it is believed by many that the height and character of a surface mixed layer is the critical factor in the dispersion of plumes and the resulting ground-level concentrations from tall stacks.

Numerical simulation is a potentially powerful tool for the study of turbulence, including the linking of the Lagrangian system, which describes diffusion most naturally, and the Eulerian system in which most data are acquired. However, a very serious problem in numerical simulation is that it is extremely difficult to simulate precisely three-dimensional turbulent flow, provide sufficient resolution at all wave numbers, and retain sufficient complexity in situations such as shear and stratification. R.L. Peskin concludes that numerical simulation of Lagrangian flow is at the present time a good research tool, but is not yet recommended for operational problems. The paper by J.L. Lumley and B. Khaejh-Nouri and that by Wyngaard et al. discuss the use of higher order closure. Second-order closure of the equations expressing the perfect gas law, continuity, momentum, energy, and pollutant concentration yields a set of equations expressed solely in terms of

the mean variables and/or their second-order correlations and renders unnecessary some external factors such as the diffusivity K. The choice of closure assumptions in the model is very critical, however, and the modelling of sub-grid turbulent motions remains a major problem.

It has been found experimentally that if one measures the turbulent velocities in a wind tunnel which has an internal boundary layer because of a change in surface roughness, and subsequently carries out a statistical analysis of these velocities, the flow is non-Gaussian. Non-Gaussianity is the subject of several papers in Volume 18A. It is suggested by Z. Zarić and also by R.A. Antonia and R.E. Luxton that non-Gaussianity is due to "intermittency," i.e. a switching back and forth at a specific location between two flows with different turbulent characteristics. Flow visualization by W.W. Willmarth and S.S. Lu using hydrogen bubbles in a water tunnel indicates that intermittency is caused by "bursts" in which slower-moving fluid from near the wall penetrates the boundary layer into the faster moving fluid. The "burst" concept is extremely interesting but it remains to be seen how it will be applied to meteorological and oceanographic problems.

Eddy diffusion coefficients are very widely used in work in environmental diffusion. F.K. Wippermann has developed a model of the atmospheric boundary layer whose predictions of vertical profiles of eddy diffusivity K as a function of mixing length compared well with field observations. An interesting feature of the K-profiles in a baroclinic boundary layer was a sharp minimum, not due to a temperature inversion but due to the baroclinicity. As in the case of a temperature inversion, however, such a K-minimum could act as a barrier to the vertical dispersion of pollutants emitted from a tall stack.

Another problem that has intrigued meteorologists is the relationship between the time scales in the Lagrangian and Eulerian frames of reference. As a result of one of his many experiments with constant volume balloons, J.K. Angell has made the comparison in the vertical dimension. Eulerian vertical velocities were obtained from Gill anemometers on a tower; Lagrangian velocities were obtained by radar tracking of balloons moving past the tower. Angell then compared the resulting ratios of Eulerian and Lagrangian time scales with those predicted by a model of "frozen turbulence" in which the eddies are represented by "cartwheels" of fixed diameter moving downwind at the mean wind speed. He found that the "frozen turbulence" model was not successful in predicting the variations of the ratio of time scales with changes in turbulent intensity and that one must take into account the decay and rebuilding of eddies as they move past the fixed instrument.

Volume 18B deals primarily with the application of turbulence theory to practical problems, rather than with theories themselves. The dispersion of atmospheric pollution on a regional and global scale is very much a matter of increasing concern at the present time and, appropriately, volume 18B begins with several papers on this important topic. F. Pasquill discusses the applicability of three main theoretical frameworks (gradient-transfer concept, statistical theory, and similarity theory) to regional dispersion problems and concludes that the vertical distribution of pollution must be considered in three main layers: a shallow surface layer containing pollution from local sources, an intermediate layer containing a near-uniform vertical distribution of pollution from more distant sources and, thirdly, the "free" atmosphere containing pollution that has been carried up beyond the boundary layer by large-scale ascent or by convective penetration. Meteorological information which is needed includes the diurnal variation of the height of the mixing layer, the rate of vertical spread of the plume in the mixing layer, and the magnitude of the large-scale vertical velocity at each stage along the trajectory. An accurate trajectory analysis is essential for the prediction of large-scale dispersion and E.F. Danielsen discusses the potential pitfalls that lurk for those who dare to venture into trajectory analyses. Errors of several *hundred* kilometres can result from using the assumption that air parcels follow surfaces of constant pressure rather than constant entropy. Results are also very sensitive to the type of wind equation that is used. Danielsen's paper is highly recommended for those contemplating trajectory analyses.

Attempts at global-scale-dispersion modelling are discussed in papers by L. Machta,

and by G. Czeplak and C. Junge. Machta reviews the current data on tracer substances such as Argon-37, Freon-11, and carbon dioxide. He uses a simple model with classical K-type diffusion. The two-dimensional distributions of various tracer substances predicted by this engineering approach are then compared with observations. Generally, he finds that the coarse features of distributions are well approximated in the troposphere by the above flux-gradient model. The best comparison is with Freon-11 because of the relative certainty of knowledge of the rate of emissions and the accuracy of observed concentrations. In fact, Machta states that one of the most pressing problems in global dispersion modelling is the lack of good observations for testing the model results.

Dispersion models have been applied to regional problems both in Europe and North America. H. Rodhe of Sweden separates the dispersion of a pollutant into three parts: the motion of the centre of gravity of the pollutant cloud; the diffusive growth of the cloud, and the rate of elimination of the contaminant from the atmosphere. The first part requires an accurate knowledge of the wind fields and the vertical displacements, a point which has been discussed by E.R. Danielsen. With respect to the second aspect of dispersion, Rodhe points out that a combination of vertical motion and vertical shear in the horizontal winds can lead to considerable horizontal dispersion. When the cloud grows to about 100 km in diameter, further growth is determined by the large-scale flow. Rodhe applies a model using 85 kPa trajectories to compute the deposition of sulphur over northern Europe. In view of the comments on trajectory analysis by E.F. Danielsen and by Rodhe himself, 85 kPa trajectories may seem a gross over-simplification. However, in the case of continually emitting sources of sulphur, the errors are much less worrisome than in the case of an instantaneous emission, as one is interested in the statistical distribution of a large number of trajectories. Rodhe estimates that 40–50% of sulphur deposition in Sweden comes from outside the country.

R.E. Munn reports that pollution from one city can influence another by analysing patterns of total suspended particulate matter and iron in the Detroit/Windsor and Sarnia/Port Huron area. He finds that when Windsor/Detroit is upwind of Sarnia/Port Huron, it contributes substantially to suspended particulates in areas just upwind of the latter cities. The reverse effect cannot be found.

P.A. Trout and H.A. Panofsky study the urban plume of sulphur dioxide from Los Angeles, assuming that the lateral dispersion is Gaussian with Pasquill's 1961 curves extrapolated to a downwind distance of 150 km! Despite this rather chancy extrapolation, their reported observations are within a factor 2 of predictions, and tend to confirm another assumption of a uniform vertical distribution of pollution within the surface mixed layer.

Because interest is rapidly increasing in the long-range transport of pollutants, especially in eastern Canada, the papers in this part of volume 18B are highly recommended.

Stepping down from the regional to the urban scale, two papers, one by H.G. Fortak and the other by P.A. Taylor, deal with the present state of the art. Taylor feels that, while turbulent transfer is not a local gradient process, that type of model is sophisticated enough for today's level of advancement and that the higher order closure models such as that of Lumley and Khaejah-Nouri described in volume 18A are too complex for micrometerological modelling. Flow over topography remains an important problem which Taylor thinks might be modelled physically, especially for street-level modelling. Despite the problems in urban modelling that include sub-grid scale effects, Taylor feels that prospects are encouraging and that by the late 1970s we may see numerical models that claim to represent the airflow around a particular city.

Because of the present difficulties referred to above in numerically modelling the flow of fluids around complicated shapes such as topography or cities, physical modelling in a wind or water tunnel is a potentially attractive alternative. The paper by S. Sethu Raman and J.E. Cernak reports their work in airflow over an urban "heat island." They were able to produce neutral, stable, and "trapping" (mixed layer topped by a stable layer) temperature stratification in the flow. The well known "urban dome" formed by the sloping base of an inversion was observed, as well as convergence of cool air into the urban heat island. Physical modelling appears to be a useful theoretical tool in studying urban-scale

dispersion of pollution. Whether or not it will be a useful "real-time" operational tool remains to be seen due to the time needed to set up the model. Perhaps the best way that physical modelling could be used operationally would be to create scenarios beforehand of critical meterological conditions.

Removal processes are crucial in completing the atmospheric cycle of pollutants. One paper in volume 18B is of particular interest—that of I.E. Galbally on gas transfer near the earth's surface. The various mechanisms of uptake at the surface and the limiting factors are discussed. The concept of gas transfer is made analogous to that of electrical resistances in series; the result is a relationship between gas uptake at the surface and wind speed and gas concentration at some height z above the surface. Information on gas uptake parameters and resistance of the viscous layer is given in this paper, which is highly recommended reading for someone wishing a grounding in gas transfer at the surface. As a general comment, I would have liked to have seen more papers on gas uptake in this volume, considering the importance of this part of the atmospheric pollution cycle.

While most of the papers in volumes 18A and 18B with atmospheric diffusion, there are several papers dealing with diffusion in the sea that will be of interest to oceanographers. The paper by K.F. Bowden et al. using tracer dye indicates that horizontal dispersion fits a Gaussian distribution with σ^2 proportional to the travel time raised to a power. K. Takeuchi and S. Ito, observing a thermal plume from a power plant, found that the lateral distribution of surface temperature could also be expressed by the Gaussian curve. Thermal plumes will be of major importance with the increased generation of electricity at plants burning fossil fuel or using nuclear energy.

G. Kullenberg studied the vertical distribution of tracer dye for travel times of over 24 hours and observed that the dye was found in several shallow homogeneous layers of 15–20 cm thickness at a depth of 50 m in the Baltic sea. The temperature structure of the water was sheet-like, i.e. isothermal layers separated by "sheets" of strong temperature gradient. Kullenberg concludes that, in the above case, vertical mixing rates are slow and intermittent and are mainly governed by shear instabilities.

The formidable problems of observing turbulence at sea from a towed sensor are discussed in a paper by C.H. Gibson et al. Millimetre spatial resolutions are needed and, for towing speeds of 1 m/s, the required frequency response is 1000 Hz. False velocities due to surface motion transmitted through the towing cable to the sensor is also a problem; high pass filtering is needed.

One alternative to observations in the sea itself is analogous to that for the atmosphere: physical modelling. M. Coantic and A. Foare describe the elaborate combination of micrometeorological wind tunnel and wind-wave tank they use to study air-sea interaction at l'Institut de Mécanique Statistique de la Turbulence. Effects of solar radiation are simulated by heating the water. They describe some results of their work: wave spectra for different fetches and the non-Gaussianity of instantaneous water levels because the wave crests are sharper than the troughs. Mean profiles of velocity, temperature, and humidity are also examined as a function of downwind distance along the tunnel. They also observed intermittent occurrence of intense turbulent "bursts," lending support to the concept described above in the papers by Zarić and by Antonia and Luxton.

In summary, volumes 18A and 18B of *Advances in Geophysics* cover a wide range of topics, with emphasis on both theoretical and applied aspects. (If this review has leaned towards the latter, it is because of the bias of the reviewer.) Technically, the two volumes are up to the usual high standard of Academic Press, with no significant errors apparent in the text or the figures. I recommend these volumes to any serious worker in environmental diffusion and hope that proceedings of future similar symposia will be as useful and interesting.

R.W. Shaw
Environmental Protection Service
Environment Canada
Halifax, N.S.

CALL FOR PAPERS – TWELFTH ANNUAL CONGRESS

The Twelfth Annual Congress and Annual General Meeting of the Canadian Meteorological and Oceanographic Society will be held at The University of Western Ontario towards the end of May, 1978. The theme of the opening session will be entitled "Energy, the Meteorologist and the Oceanographer" as presented by invited and contributed papers. Subsequent sessions will deal with contributed papers on meteorology and oceanography, including sessions of common interest according to the papers submitted.

Titles and definitive abstracts (less than 300 words) should reach the program committee by *1 February, 1978.* Papers on meteorology should be sent to Prof. D.R. Hay, Department of Physics, The University of Western Ontario, London, Ont. N6A 3K7. Papers on oceanography should be sent to Mr. Farrell M. Boyce, Canada Centre for Inland Waters, 867 Lakeshore Road, Burlington, Ont. L7R 4A6.

APPEL DE TEXTES – DOUZIEME CONGRES ANNUEL

Le douzième congrès annuel et l'assemblée générale annuelle de la Société canadienne de météorologie et d'océanographie auront lieu à l'Université Western Ontario vers la fin de mai 1978. Les présentations de la session d'ouverture traiteront du thème "L'énergie, le météorologiste et l'océanographe" tandis que les autres sessions seront consacrées aux présentations ayant trait à divers aspects de la météorologie et l'océanographie, incluant des sessions d'intérêt commun, selon les papiers soumis.

Les titres ainsi que les sommaires définitifs (maximum 300 mots) devront parvenir au comité du programme d'ici le *1er février 1978.* Les textes en météorologie devront être envoyés au professeur D.R. Hay, Département de Physique, l'Université Western Ontario, London, Ontario, N6A 3K7, tandis que ceux traitant d'océanographie devront être expédiés à M. Farrell M. Boyce, Centre Canadien des Eaux Intérieures, 867 Lakeshore Road, Burlington, Ontario, L7R 4A6.

INFORMATION FOR AUTHORS

Editorial policy. *Atmosphere* is a medium for the publication of the results of original research, survey articles, essays and book reviews in all fields of atmospheric science. It is published quarterly by the CMS with the aid of a grant from the Canadian Government. Articles may be in either English or French. Contributors need not be members of the CMS nor need they be Canadian; foreign contributions are welcomed. All contributions will be subject to a critical review before acceptance. Because of space limitations articles should not exceed 16 printed pages and preferably should be shorter.

Manuscripts should be submitted to: *Atmosphere*, Dept. of Geography, University of British Columbia, 2075 Wesbrook Mall, Vancouver, British Columbia, V6T 1W5. Three copies should be submitted, typewritten with double spacing and wide margins. Heading and sub-headings should be clearly designated. A concise, relevant and substantial abstract is required.

Tables should be prepared on separate sheets, each with concise headings.

Figures should be provided in the form of three copies of an original which should be retained by the author for later revision if required. A list of legends should be typed separately. Labelling should be made in generous size so that characters after reduction are easy to read. Line drawings should be drafted with India ink at least twice the final size on white paper or tracing cloth. Photographs (halftones) should be glossy prints at least twice the final size.

Units. The International System (SI) of metric units is preferred. Units should be abbreviated only if accompanied by numerals, e.g., "10 m," but "several metres."

Footnotes to the text should be avoided.

Literature citations should be indicated in the text by author and date. The list of references should be arranged alphabetically by author, and chronologically for each author, if necessary.

RENSEIGNEMENTS POUR LES AUTEURS

Politique éditoriale. *Atmosphère* est un organe de publication de résultats de recherche originale, d'articles sommaires, d'essais et de critiques dans tous les domaines des sciences de l'atmosphère. Il est publié par la SMC à l'aide d'une subvention accordée par le gouvernement canadien. Les articles peuvent être en anglais ou en français. Il n'est pas nécessaire que les auteurs soient membre de la SMC; les contributions étrangères sont les bienvenues. A cause des limitations d'espace les articles ne doivent pas dépasser 16 pages dans le format final. Tout article sera soumis à un critique indépendant avant d'être accepté.

Les manuscrits doivent être envoyés à: *Atmosphère*. Dép. de géographie, Université de la Columbie-Britannique, 2075 Wesbrook Mall, Vancouver, La Columbie-Britannique, V6T 1W5. Ils doivent être soumis en trois exemplaires dactylographiés à doubles interlignes avec de larges marges. Les titres et sous-titres doivent être clairement indiqués. Chaque article doit comporter un résumé qui soit concis, pertinent et substantiel.

Les tableaux doivent être préparés et présentés séparément accompagnés d'un titre concis et d'un numéro.

Les graphiques doivent être présentés en trois copies dont les originaux devraient être conservés par l'auteur au cas où ils seraient nécessaire de les reviser. Une liste des légendes des graphiques doit être dactylographiée séparément. L'étiquettage doit être de grand format de façon à ce qu'il soit facilement lisible après réduction du format. Le traçage des lignes doit s'effectuer au moyen d'encre de chine en doublant, au moins, le format final, le tout sur papier blanc ou sur papier à calquer et identifié adéquatement. Les photographies (demi-teintes) devraient être présentées sur épreuves glacées au double du format final.

Les unités. Le Système International (SI) d'unités métriques est préférable. Les unités devraient être abrégées seulement lorsqu'elles sont accompagnées de nombres, ex: "10m," mais "plusieurs mètres."

Les notes de renvoie au texte doivent être évitées.

Les citations littéraires doivent être indiquées dans le texte selon l'auteur et la date. La liste des références doit être présentée dans l'ordre alphabétique, par auteur et, si nécessaire, dans l'ordre chronologique pour chaque auteur.

The Canadian Meteorological Society / La Société météorologique du Canada

The Canadian Meteorological Society came into being on January 1, 1967, replacing the Canadian Branch of the Royal Meteorological Society, which had been established in 1940. The Society exists for the advancement of Meteorology, and membership is open to persons and organizations having an interest in Meteorology. At nine local centres of the Society, meetings are held on subjects of meteorological interest. *Atmosphere* as the scientific journal of the CMS is distributed free to all members. Each spring an annual congress is convened to serve as the National Meteorological Congress.

Correspondence regarding Society affairs and CMS membership should be directed to the Corresponding Secretary, Canadian Meteorological Society, c/o Dept. of Geography, Simon Fraser University, Burnaby, B.C., V5A 1S6.

There are three types of membership – Member, Student Member and Sustaining Member. For 1977 the dues are $20.00, $5.00 and $60.00 (min.), respectively. The annual Institutional subscription rate for *Atmosphere* is $15.00.

Correspondence relating to institutional subscriptions should be directed to the University of Toronto Press, Journals Department, 5201 Dufferin St., Downsview, Ontario, Canada, M3H 5T8. Cheques should be made payable to the University of Toronto Press.

La Société météorologique du Canada a été fondée le 1er janvier 1967, en replacement de la Division canadienne de la Société royale de météorologie, établie en 1940. Cette société existe pour le progrès de la météorologie et toute personne ou organisation qui s'intéresse à la météorologie peut en faire partie. Aux neuf centres locaux de la Société, on peut y faire des conférences sur divers sujets d'intérêt météorologique. *Atmosphère*, la revue scientifique de la SMC, est distribuée gratuitement à tous les membres. A chaque printemps, la Société organise un congrès qui sert de Congrès national de météorologie.

Toute correspondance concernant les activités de la Société et les souscriptions à la SMC devrait être adressée au Secrétaire-correspondant, Société météorologique du Canada, Département de Géographie, L'Université Simon Fraser, Burnaby, B.C., V5A 1S6.

Il y a trois types de membres: Membre, Membre-étudiant, et Membre de soutien. La cotisation pour 1977 est de $20.00, $5.00 et $60.00 (min.) respectivement. Les institutions peuvent souscrire à *Atmosphère* au coût de $15.00 par année.

La correspondance concernant les souscriptions des institutions doit être envoyée aux Presses de l'Université de Toronto, Département des périodiques, 5201 rue Dufferin, Downsview, Ontario, Canada, M3H 5T8. Les chèques doivent être payables aux Presses de l'Université de Toronto.

Council / Conseil d'administration 1977–78

President/Président – K.F. Harry
Vice President/Vice-Président – R.W. Burling
Past President/Président sortant – J.E. Hay
Corresponding Secretary/Secrétaire-correspondant – R.B. Sagar
Treasurer/Trésorier – D.G. Schaefer
Recording Secretary/Secrétaire d'assemblée – P. Sagert
Councillors-at-large/Conseillers – F. Dobson, E. Einarson, H.L. Ferguson
Chairmen of Local Centres/Présidents des centres

ATMOSPHERE

Editor/Rédacteur – J. Derome
Associate Editors/Rédacteurs adjoints – C. East, J.B. Gregory, W. Gutzman, P.H. LeBlond, R. List, C.L. Mateer, G.A. McBean, D.N. McMullen, P.E. Merilees, R.R. Rogers, V.R. Turner, R.E. Thomson, E.J. Truhlar, E. Vowinckel